Automatic Slip Controller for Railway Vehicles Using Fuzzy Logic

Emebet Gebeyehu Gedlu

A Thesis Submitted to

The School of Electrical and Computer Engineering

Presented in Fulfillment of the requirements for the Degree of Master of Science (Electrical Engineering for Railway Systems)

Addis Ababa University

Addis Ababa, Ethiopia

July 2017

Addis Ababa University

Addis Ababa Institute of Technology

School of Electrical and Computer Engineering

This is to certify that the thesis prepared by Emebet Gebeyehu, entitled: *Automatic slip controller for railway vehicles using fuzzy logic* and submitted in partial fulfillment of the requirements for the Degree of Master of Science (Electrical Engineering for Railway Systems) complies with the regulations of the university and meets the accepted standards with respect to originality and quality.

Signed by Examining Committee:

Examiner_____ Signature_____ Date_____

Examiner_____ Signature_____ Date_____

Advisor_____ Signature_____ Date_____

Advisor_____ Signature_____ Date_____

Declaration

I, Emebet Gebeyehu, declare that this thesis is my original work, has not been presented for a degree in this or other universities. All sources of materials used for this thesis work have been fully acknowledged.

Name: Emebet Gebeyehu Signature: _____

Place: Addis Ababa University, Addis Ababa

Date of Submission: _____

This thesis has been submitted for examination with my approval as a university advisor.

Mr Abebe Demise Signature:

Advisor's Name _____

Abstract

The moment applied on the wheel by the traction motor has to be transferred in to tangential force in order to guarantee the longitudinal motion of train vehicle. The force that is transmitted between wheels and rail is called the adhesion force which is the product of normal force and adhesion coefficient. The adhesion coefficient depends on the slip velocity, conditions of rail surface, a train velocity and temperature in the contact area. From parameters that can influence the adhesion coefficient slip velocity the vital one. Therefore slip controlling is important in order to prevent wear of the wheels and the rail and to use the present adhesion effectively.

On this thesis the relation between the wheel road adhesion force coefficient and slip ratio is developed based on Burckhardt Static Modell (BSM) which treats the wheel as a circular beam supported by springs. First the longitudinal slip ratio is to be calculated as the speed difference of the driven and non-driven wheels. Where, the non-driven wheel presents speed of the train vehicle and the driven wheel velocity is considered as the wheel-rail contact specimen. Then adhesion torque observer is designed in order to estimate the existing adhesion in real time. This torque is then applied as a load torque for Proportional Integral (PI) controller based speed loop.

After developing proper speed loop to control wheel speed, Fuzzy Logic Controller (FLC) based slip controller is installed inside to compensate traction torque fluctuation caused by adhesion load. The FLC has two inputs namely the slip ratio error and the rate of slip ratio error. Using linguistic rules to increase and decrease compensating torque, the FLC generates adhesion coefficient which will be multiplied by the normal force and wheel radius to be added or subtracted from the traction torque.

Then the advantage of the controller is evaluated by considering the speed response with and without the slip controller. For the slip ratio varying drastically from 0.7 to 0.01 and vice versa, the wheel speed response shows up to 50% overshoot and undershoot in the early stage of the accelerating speed. However, the FLC slip controller compensates this up and down to 6% which is a remarkable result to smooth the motion of the system.

Key words: - Slip, Adhesion coefficient, Fuzzy logic controller (FLC), Proportional Integral (PI)

Acknowledgment

For the successful completion of this thesis work, my first gratitude goes to my parents Mr. Gebeyehu Gedlu and Mrs. Mulu Asefa for their attentive appreciation and support.

Then it is my greatest pleasure to thank my advisor Mr. Abebe Demissie for his enormous support on technical and nontechnical subjects to bring this thesis work alive.

Lastly, but not the least, my thanks goes to my friend Yared Kassahun for his support since the start this masters study.

Table of Contents

List of Figures

List of Tables

List of Symbols and Abbreviations

List of Symbols

R_w Radius of the wheel,

ω Angular velocity of the wheel and

V Longitudinal velocity of the vehicle.

λ Slip ratio

V_s Slip velocity

F_a Adhesive force

μ_a Adhesion coefficient,

N Normal force,

m_a Adhesive mass of the vehicle and

g Gravitational constant.

T Motor torque

T_L Load torque

J Inertia

p Contact pressure

x_c Displacement from the tip of contact footprint

l Length of the contact footprint

w Width of the contact footprint

C_x Modulus of transverse elasticity,

l_h Displacement at which the adhesion force derivative fx changes rapidly,

μ_d Dynamic friction coefficient.

μ_{max} Maximum adhesion coefficient,

a Constant that determines the dynamic friction coefficient in the slipping reign,

K_x Traveling stiffness

B Viscous friction torque between the motor shaft and the wheel

T_a	Adhesion torque
$\dot{V}$	Acceleration of the train
F_a	Adhesion force
F_t	Tractive force
F_r	Disturbance force
τ	Time constant of the adhesion torque observer
K_p	Proportional term constant
K_i	Integral term constant
ζ	Damping constant,
ω_n	Natural frequency
C_1	Maximum value of friction curve
C_2	The friction curve shape
C_3	The friction curve difference between the maximum value at λ=1

List of Abbreviations

FLC	Fuzzy Logic Controller
SBM	Static Beam Model
PID	Proportional-Integral-Derivative
FIS	Fuzzy Inference System
NB	Negative Big
NS	Negative Small
ZO	Zero
PB	Positive Big
PS	Positive Small
FS	Fuzzy Set

Chapter One

Introduction

1.1 Background

The kinematic principle of any wheeled vehicle is that, the moment torque applied on the circular disc have to produce a horizontal sheer which enables a forward motion instead of rotating at a fixed position [1]. In order to have a force transfer from a perpendicular direction in to horizontal one, the contact between the wheel and the surface it rotates on must be granted. The mechanical force due to the contact between two surfaces can be defined as adhesion force, which is the transmitted tangential force in the longitudinal direction between the wheel and rail in case of railway vehicles. Adhesion force is highly dependent on the normal load of the railway vehicle and adhesion coefficient, which is determined by mechanics property of particles at the contacting area [2]. Generally adhesion force is important over acceleration and deceleration motion of any railway vehicle. For example, low adhesion during braking will extend the braking distance, which causes a safety issue. Low adhesion during driving reduces the acceleration, leading to timetable disruption. If the adhesion is too high, wheels and rails are subject to excessive shear stress, leading to severe wear and surface fatigue [3].

It has been demonstrated that the adhesion force is a function of adhesion coefficient, which is again highly depends on relative longitudinal speed of the wheel and the vehicle, called slip. Slip ratio is the normalized relative longitudinal speed of the wheel and the railway which is extremely complicated, rapidly changing and it is caused by certain and uncertain forces acting on the train [3,4].

Slip control was traditionally considered as part of the maneuvering and braking system, but it has important relationships with the train control system. This thesis is researched to design an automatic slip controller using a Fuzzy Logic Controller (FLC) in order to achieve optimized adhesion force between railway vehicle wheel and railroad. Before designing a controller, it is important to represent train and wheel-rail contact models mathematically. Among different models of wheel-rail contact, Burckhardt Static Modell (BSM) is selected because of its easy representation and less use of continuum mechanics parameters [5].

Because of the relation between slip and adhesion coefficient is a non-linear, time varying process, a non-linear controllers like FLC are well suited. One major advantage with FLC is that it can include experienced human experts linguistic rules, to design the slip control system which can keep adhesion constant optimal. These linguistic rules are especially important when the access to measured data is limited [6]. The reason is that they often contain information that is not included in the numerical values. These rules can be translated into if-then rules and in this form be included in the fuzzy logic algorithm.

As a matter of fact, lots of researches are done on this specific area as discovered during this thesis development i.e. it will be discussed on literature review section. On this work, the FLC keeps the slip ratio to a constant value which is found to provide maximum adhesion coefficient. The effect of this method is verified by contending the slip controller inside the classical PI controller based speed loop to compensate traction torque in order to improve speed response of traction motor.

1.2 Statement of the Problem

The moment applied on the wheel by the traction motor has to be transferred in to tangential force in order to guarantee the longitudinal motion of train vehicle. The force that is transmitted between wheels and rail is called the adhesion force. The tangential force is transmitted by a small contact area between the wheel and rail having area of a few micro square centimeters. The maximum value of the tangential force depends on the adhesion coefficient and the locomotive adhesion weight. The adhesion coefficient depends on the slip velocity, conditions of rail surface, a train velocity and temperature in the contact area. From parameters that can influence the adhesion coefficient only the train velocity and slip velocity can be changed and controlled.

Slipping of wheels on the rail at time of adhesion loss causes sharp variation of the load torque. This means the coupling between the electric motor torque and the train inertia disappears instantaneously. The motor load moment is reduced to only the transmission inertia of axles and wheels, which is several orders of magnitude smaller than the train's nominal inertia. In order to avoid this problem, we need to control the slip ratio to a value which gives maximum adhesion coefficient.

The goal of all slip control methods is to control the slip in order to prevent wear of the wheels and the rail and to use the present adhesion effectively. Optimizing methods also adds a search of the maximum adhesive force. This is achieved when the slip is controlled towards the peak of the slip adhesion relation. To be able to do this, three major problems must be solved:

- The existing adhesion must be known
- The slip present must be detected.
- The slip must be controlled towards the optimal slip which gives maximum adhesion.

Because of the relation between slip and adhesion force are a lot more complex than they might seem at first, this research work studies their relation and designs a controller.

1.3 Objective/Aim of the Study

1.3.1 General Objective

The general objective of this research is to design an automatic slip controller using FLC to retain maximum adhesion force between the wheel and the rail which can improve speed response of classical PI speed controller.

1.3.2 Specific Objectives

- To thoroughly study different slip controlling mechanisms
- Developing mathematical model which relates the slip and adhesion constant of rail vehicle.
- Design slip and adhesion coefficient estimator which can trace these parameters in real time.
- Design and implement FLC inference algorithm by properly assigning input and output membership functions.
- Simulate and analyze the speed loop with and without a slip controller on MATLAB Simulink.

1.4 Scope of the Thesis Work

Controlling slip is a vast concept depending on the type of input, output, controlling variables, and the degree of freedom the motion of the train to be considered. The delimitations of this work is based on the following boundaries.

1. Only the longitudinal motion of the train is considered, disturbances such as curving, wind resistance and gradient are considered as cause of slip velocity (relative longitudinal speed between the wheel and train vehicle).
2. Only one wheel-rail contact, loading and response is analyzed.
3. The radius of the wheel is assumed as rigid and constant with small sleeping footprint
4. Only the wheel-rail dynamics is modelled and the train modelling is not under the scope of this work

1.5 Methodology

The below water fall diagram shows how the research has been carried out. Each step will have its own time boundary and detailed procedure.

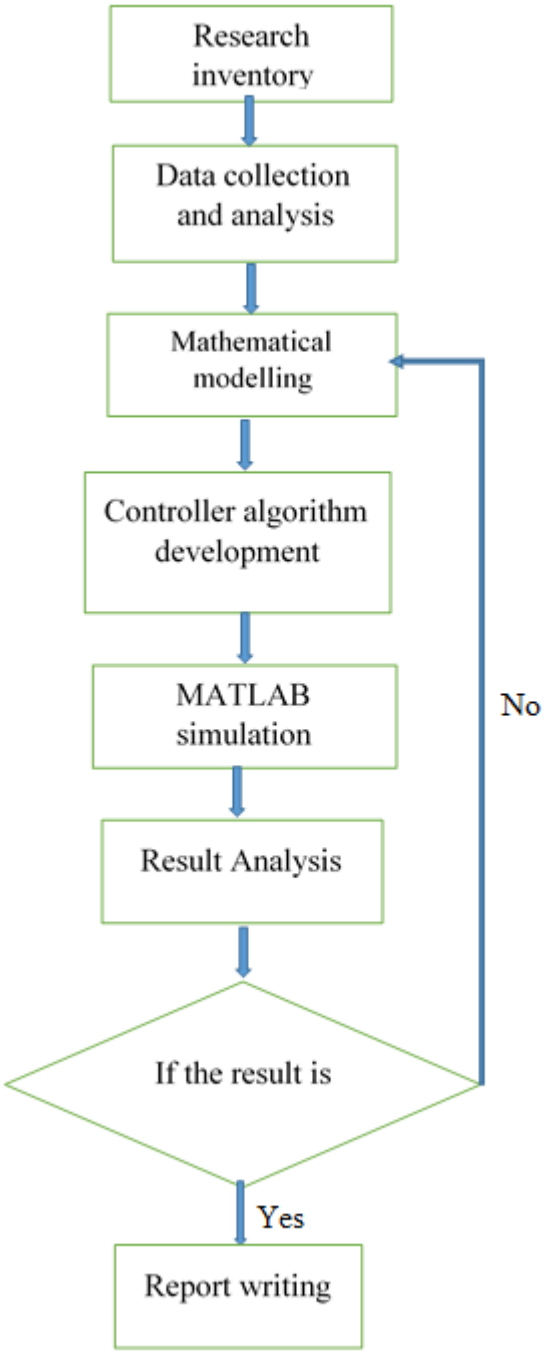

Figure 1.1 Water Fall Diagram of Methodology

1.5.1 Data Inventory

The purpose is not only to get the necessary background knowledge, and also to find approaches of automatic slip control that can be applied for railway vehicles. On this phase of the thesis, different books, blogs, publications, journals etc. are primarily addressed in order to have the insight of the existing slip controller. Moreover, discussion and getting advises from the professors is the crucial action.

1.5.2 Data Collection and Analysis

After distinguishing the source of data, they are merged and wrapped up as per their importance and type of classification. To do with the simulation and implementation, different parameter data need to be collected on the process of operation. The train profile and controlling system in detail is also required from the train manufacturers or from the operation manual. The research needs also how often the wheel and drive systems are changed due to slip/slide problems. Then assessing the weakness of the existing system, calculating and organizing technical & operational Requirements will be held. This type of research is explanatory type of research. Since, it is based on previous research experiments and intervention studies which means all the data/parameters used in this research are collected and based on some other mathematical algorithms and formulations of previous work. At the beginning of this work, it has been intended to use practical parameters from Addis Ababa Light Rail Transport (AALRT). However, it has been difficult to find material related data from the administering institution. Therefore, data from internet is used from related works done.

1.5.3 Mathematical Modelling

Though the relation between wheel and rail vehicle is complicated, mathematical model for maximum adhesion-slip relation is developed based on Burckhardt Static Modell (BSM) which treats the wheel as a circular beam supported by springs. First the longitudinal slip ratio is to be calculated as the speed difference of the driven and non-driven wheels. Where, the non-driven wheel presents speed of the train vehicle and the driven wheel velocity is considered as the wheel-rail contact specimen. Then adhesion torque observer is designed in order to estimate the existing adhesion in real time. This torque is then applied as a load torque for PI controller based speed loop.

1.5.4 Controller Algorithm Development

Based on adhesion sleep and adhesion observer mathematical models, the controller determines the optimum slip to get the proper adhesion. The FLC determines how much the speed of the wheel should lead or lag train's speed based on the collected data and their relationship in the mathematical model. The Fuzzy Inference System (FIS) rules and membership functions are organized based on Mamandi's linguistic relations.

1.5.5 MATLAB Simulation

Models and algorithms developed are simulated on Simulink environment by assigning values to equation variables. Then a step input change is applied to adhesion force, and the response of the system to the change is graphically demonstrated and analyzed for the speed loop with and without slip controller.

1.6 Thesis Contribution

This thesis work is a cautious study of the improving railway vehicle dynamics by controlling slip ratio. It is anticipated that it will have main contribution on the following aspects.

- It will give clear understanding of the slip ratio and adhesion coefficient and their relationship
- It will point out which parameters are important in relation to rail and wheel materials property and structural architecture.
- It will show how fuzzy controllers are designed and implemented

1.7 Thesis Organization

As a general report of the thesis work, this paper is consisting of five chapters. Chapter one is introduction of the report with unanimous descriptions and summary. This chapter has six subtitles namely, background, statement of the problem, objective, methodology and thesis contribution.

Chapter two is literature review, which is a collection of theoretical backgrounds on which an automatic slip controller design is founded on. On theoretical background part, wheel-rail contact mechanics and the relation between adhesion force and slip ratio is studied. Moreover, related works are described to show which methods are followed on this work and what makes it different. Chapter there is about mathematical modelling, which is the main part of the thesis. Theoretical backgrounds studied under chapter two are verified using numerical values and arranged in a system level. Adhesion torque observer, wheel rail contact, slip ratio, PI controller based speed loop and slip controller using FLC are modelled in this part.

Chapter four is about MATLAB simulation. After the development of MATLAB Simulink Model depending on the mathematical models developed in chapter three. The simulation result for the models will be discussed and described in terms of performance improvement.

The final chapter is recommendation and conclusion. Here, the thesis work concluded based on the result obtained and discussed in chapter four. Further recommendation for the development of new model or improvement of the result in this thesis is suggested

Chapter Two

Literature Review

2.1 Theoretical Background

2.1.1 Wheel-Rail Contact

In railway vehicles, the applied tractive effort to drive its wheels should provide longitudinal motion. When a torque is applied to a circular wheel, it doesn't roll, but actually rotates faster than the corresponding longitudinal velocity of the vehicle. This causes the deformation of the circular wheel at the rail contacting point, as shown on Fig 2.1, and shifts the normal force in to horizontal sheer. This is the horizontally shifted force, which makes the railway vehicle move forward [1].

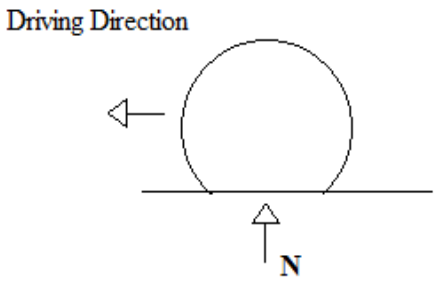

Figure 2.1 Sleeping of a wheel

Due to certain and uncertain forces applied on both objects (train and wheel), usually they tend to have different speeds. This difference between the longitudinal velocity of the wheel and the corresponding longitudinal velocity of the vehicle is defined as slip velocity. Usually this difference is normalized by vehicle speed and called slip ratio as shown on equation 2.1.

$$\lambda = \frac{\omega R_w - V}{V} \tag{2.1}$$

Where, R_w is the radius of the wheel,

ω is the angular velocity of the wheel and

V is the longitudinal velocity of the vehicle.

λ is slip ratio

The numerator of equation 2.1 can be defined as slip velocity V_s

$$V_s = \omega r - V \tag{2.2}$$

Sometimes, a separate definition of the slip is used when the slip velocity is negative. This is often called slide. On this thesis report, it is referred as negative slip.

What makes the wheel of the railway vehicle slip?

It is due to the massive weight of the railway vehicle, both the wheels and the rails expands and contracts in different regions when wheels are driven. This contraction and expansion causes the small slip to occur. In order to keep this small slipping of wheels over the rail road, we have to make sure there is always a contact between them. This force of attachment between two contacting objects is defined as adhesive force [9]. It will be the ability of the wheel to exert the maximum tractive force on the rail and still maintain persistence of contact without exceeding the optimal limit. The adhesive force is given by

$$F_a = \mu_a N = \mu_a m_a g \tag{2.3}$$

Where F_a is the adhesive force

μ_a is the adhesion coefficient,

N is the normal force,

m_a is the adhesive mass of the vehicle and

g is the gravitational constant.

The adhesive mass is defined by the total mass on all the driven wheels. F_a changes in time, though the normal force N is constant, which implies that the adhesion coefficient μ_a changes in time. There are several factors that affect the value of the adhesion coefficient but the most significant ones are contaminants, vehicle velocity and slip velocity [10].

Contaminants: - due to the very high stress at the wheel-rail contact point, high adhesion levels could be obtained. Due to high stress, molecular levels of contaminants can lower the adhesion considerably. Also larger amount of contaminants like oil, leaves and moister lead to major reduction in adhesion. These factors are random and are therefore hard to model but it is crucial to consider them with random disturbance [10].

Vehicle velocity: - as the wheels roll along the track, they bounce on surface irregularities. This reduces the normal force between the wheel and the track. If the normal force decreases, so will the adhesive force. In general, it can be said that the adhesive force is reduced with increasing vehicle velocity [11].

Slip velocity: - the slip velocity is the most important factor influencing adhesion. The adhesion coefficient can becomes higher if the slip velocity is controlled effectively [10][11]. As described earlier, some slip is required in order to transfer the motor torque to vehicle movement. The adhesive force increases when the slip increases, as long as the slip does not become too large. Measurements recently done by [12] confirms that the adhesion coefficient has a peak at a certain slip velocity. This is often presented in figures similar to Figure 2.2. In this figure, the region to the left of the peak is referred to as the stable region, while the right side is called the unstable region.

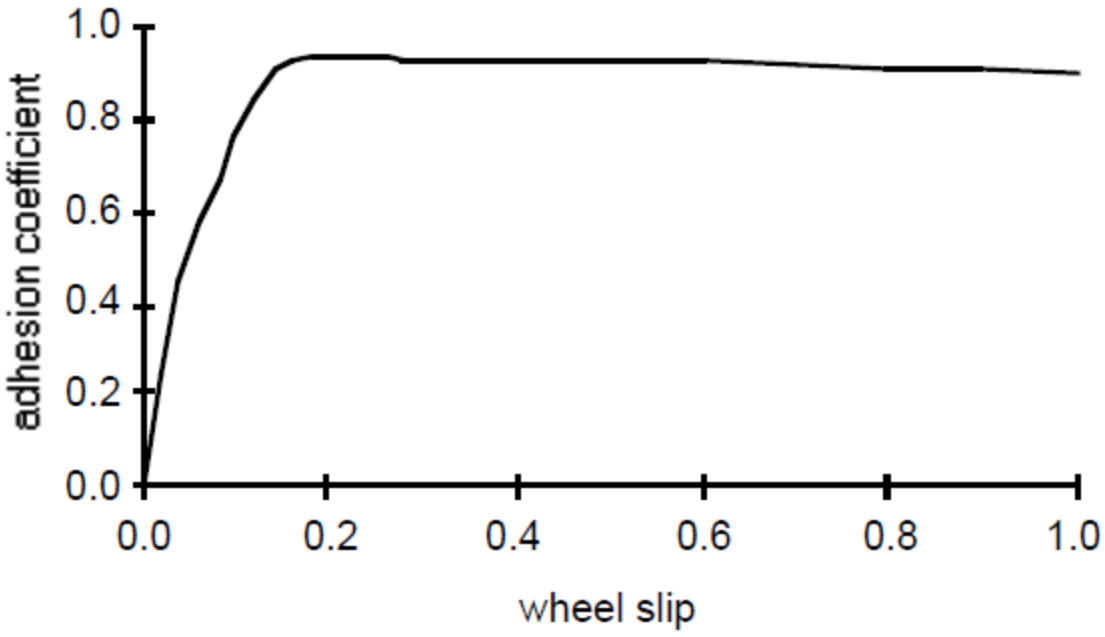

Figure 2.2 How Adhesion between Rail and Wheel Varies According to Slip [Reference]

Why we want to secure the rail-wheel contact by controlling the slip?

The speed of the train is supposed to vary from zero up to maximum operating speed to transport passengers and goods. During this process, the speed of the traction is controlled by controlling the angular speed of traction motors.

The simple kinematic law of mechanics leads to controlling a motor by the torque to overcome a load moment and to accelerate or to slow down on inertia, thus making it possible to vary its mechanical angular speed to reach quickly, and then to maintain a new speed or a new position. The position or the speed references are transformed by the control action into an acceleration reference, which makes it possible to fix the motor torque set-point [13]. This phenomenon can be expressed using mathematical equation 2.4.

$$T = J\frac{d\omega}{dt} + B\omega - T_L \tag{2.4}$$

Where T is the motor torque

T_L is load torque

J is inertia

ω is angular speed

Whatever the application, an electric motor is thus controlled initially with its torque characteristics. According to the motor type and the regulation mode, to obtain this torque, it is necessary to control the voltage/current, the magnetic field and/or the frequency of the motor supply based on its type [14].

Slipping and sliding of wheels on the rail at time of adhesion loss causes sharp variation of the load T_L. This means the coupling between the electric motor torque and the train inertia disappears instantaneously. The motor load moment is reduced to only the transmission inertia of axles and wheels, several orders of magnitude smaller than the train's nominal inertia.

2.1.2 Adhesion Coefficient and Slip

2.1.2.1 Static-Beam-Model (SBM)

As Figure 2.3 shows a simplified contact model for the rail and wheel, can be represented using Static-Beam-Model (SBM) the wheel as a circular beam supported by springs. This modelling is usually used to model automobile tire-road contact. The portion of a vehicle tire forms a contact patch, which is the actual contact with the road surface. The term footprint is also used almost synonymously. The contact footprint of an automobile tire is generally approximated as a rectangle by the beam model. In similar manner, the contact footprint between the rail and the wheel is approximated by a rectangle with highly reduced length and width dimensions, see Figure 2.3.

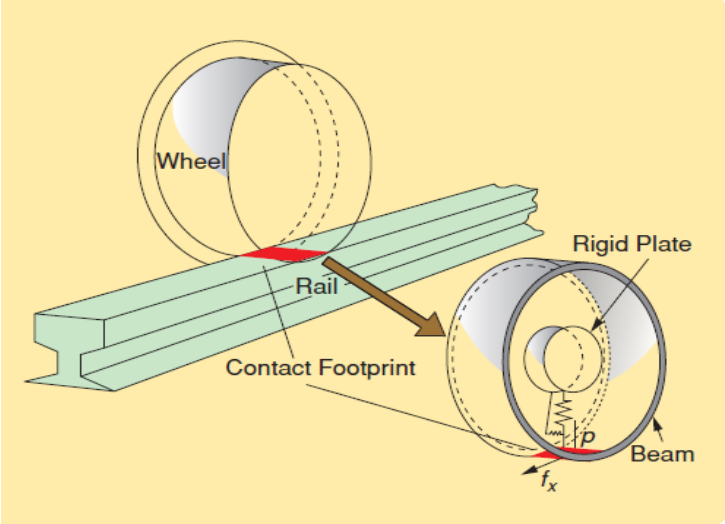

Figure 2.3 SBM for Wheel-Rail Contact [8]

The contact pressure between the rail and the wheel at the displacement from the tip of the contact footprint (see figure 2.4) in the longitudinal direction of train movement is given by equation 2.5.

$$p = \frac{6N}{l^3 w}\left[\left(\frac{l}{2}\right)^2 - \left(x_c - \frac{1}{2}\right)^2\right] \tag{2.5}$$

Where p is contact pressure

x_c is the displacement from the tip of contact footprint

N is the normal force

l is the length of the contact footprint

w is width of the contact footprint

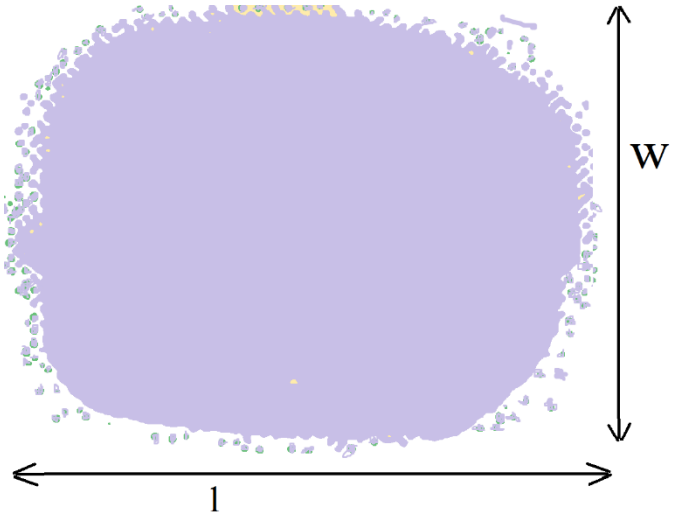

Figure 2.4 Rail-Wheel Contact Footprint [Reference]

The variablef_x, which is the derivative of adhesion force F_a with respect to the displacement x_c from the tip of the contact footprint, is highly dependent on the continuum mechanical property of the rail road. [8][4]

$$f_x = C_x w x_c \quad for\ 0 \le x_c \le l_h \tag{2.6}$$

$$= \mu_d P \quad for\ l_h < x_c \le l$$

Where C_x is the modulus of transverse elasticity,

l_h is the displacement at which the adhesion force derivative fx changes rapidly,

μ_d is the dynamic friction coefficient.

Modulus transverse elasticity is determined by civil engineering design of landing surface on which the steel rail road is installed. Whereas dynamic friction coefficient is empirical property of the contacting materials which mainly determines kinetic friction.

In particular, μ_d is defined by

$$\mu_d = \mu_{max} - \frac{a\lambda V l}{(l - l_h)} \tag{2.7}$$

Where μ_{max} is the maximum adhesion coefficient,

a is a constant that determines the dynamic friction coefficient in the slipping reign,

l_h is expressed as

$$l_h = l\left(1 - \frac{K_x \lambda}{3\mu_{max} N}\right) \tag{2.8}$$

Where K_x is traveling stiffness calculated by

$$K_x = \frac{1}{2} C_x l^2 \tag{2.9}$$

And the maximum adhesion can be given as

$$\mu_{max} = \frac{7.5}{V+44} + 0.161 \tag{2.10}$$

The wheel load, which is the normal force of the train vehicle, is equal to the integrated value of the contact pressure between the rail and the wheel over the contact foot print area. Therefore the adhesion force F_a between the rail and the wheel can be calculated by integrating fx over the length of the contact footprint and substituting the equations 2.7 to 2.10. Then, the final expression of the adhesion force in terms of slip and adhesion coefficients will become expressed as equation 2.11 [15].

$$F_a = \int_0^l f_x \, dx_c$$

$$F_a = \int_0^{l_h} C_x w x_c \, dx_c + \int_{l_h}^{l} \mu_d P \, dx_c$$

$$F_a = \frac{1}{2} C_x w l_h^2 + \mu_d \int_{l_h}^{l} \frac{6N}{l^3 w} \left[\left(\frac{l}{2}\right)^2 - \left(x_c - \frac{1}{2}\right)^2\right] dx_c$$

$$F_a = \frac{1}{2} C_x w l_h^2 + \mu_d \frac{6N}{l^3 w} \left[\frac{1}{2} l (l - l_h)^2 - \frac{1}{2} (l - l_h)^3\right] \tag{2.11}$$

However, equation (2.11) is highly material dependent and in very complicated to present adhesion force coefficient and slip ratio relationship.

2.1.2.2 Magic formula

Magic formula developed by Pacejka has been widely used to calculate steady state tire force and moment characteristics. The semi-empirical tire model combined slip situation from a physical view point. This model has been shown to suitably match experimental data, obtained under particular conditions of constant linear and angular velocity [16].

$$\mu(\lambda) = c_1 \sin(c_2 \arctan(c_3\lambda - c\_4(c_3\lambda - \arctan(c_3\lambda)))) \tag{2.12}$$

Similarly, in 1993, Burckhardt modelled, the velocity dependent braking effort coefficient between the tire and the road which has the following form

$$\mu(\lambda) = \left[C_1\left(1 - e^{-C_2\lambda}\right) - C_3\lambda\right]e^{-C_4 v_t} \tag{2.13}$$

Where

C_1 is the maximum value of friction curve

C_2 is the friction curve shape

C_3 is the friction curve difference between the maximum value at λ

C_4 is wetness characteristic value

These parameters may different for different wheel-road conditions. This modelling method is used in this thesis since it can accurately represent measured characteristics found by Kawamura [12]. More than all, it is possible to see the effect of slip ratio on adhesion coefficient by considering $C_4 = 0$.

2.1.3 Controlling Mechanisms

There are several works done to detect and control slip of a railway vehicle. Some methods are divided based on target vehicles, principle of operation, input and output parameters and desired state variables. Most of slip control methods are based on the slip velocity control, though determination of the true slip velocity is difficult because of measuring train velocity is difficult. Therefore newly developed methods like torsion, vibration or noise are under research [17].

A. Methods Based on Slip Velocity Control to a Constant Value

The methods are based on control of the slip velocity at a constant value. The methods are based on assumption that the maximum value of the adhesion coefficient occurs approximately at the same slip velocity.

The longitudinal velocity is typically determined as a velocity of the slowest wheelset or a pseudo axle is used [18]. In some cases the velocity can be determined by measuring on non-driven wheelsets. The method block diagram is in Fig. 2.5. The method can fail when the adhesion-slip velocity characteristic has a plateau and low adhesion coefficient or when all wheels has the same high slip velocity [19]. On this thesis work, this method is implemented with FLC as a slip controller.

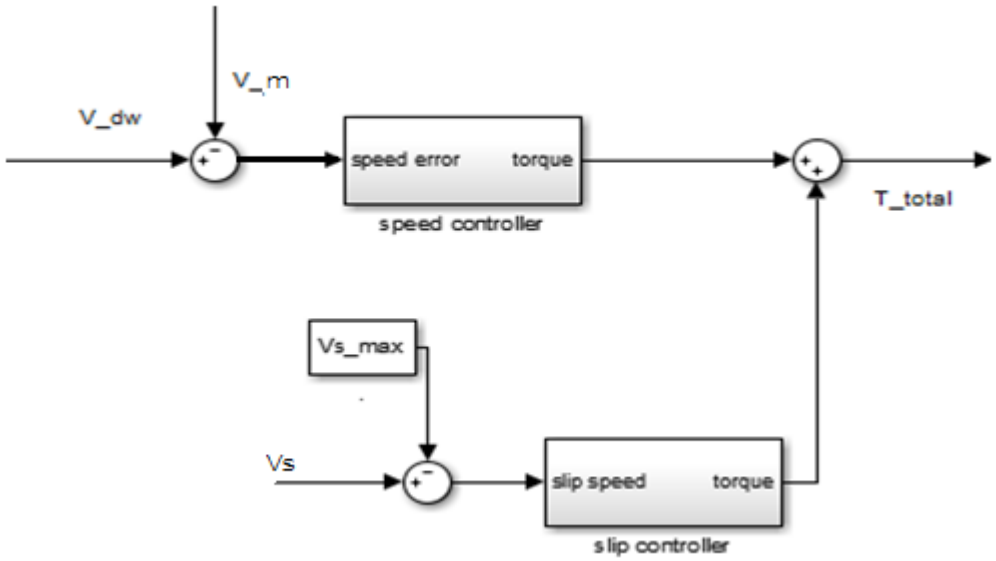

Figure 2.5 Constant Slip Velocity Control Method

B. Methods Based on Searching Maximum Value of the Adhesion Slip-Velocity Characteristic

Methods in this group control the slip velocity to achieve the peak on the adhesion-slip characteristic. Most of the methods are based on principle that the derivation of the tangential force or adhesion coefficient changes sign when the operating point moves over the maximum point on the characteristic [20].

In some cases the characteristic can have a plateau instead of peak and the methods can fail because the sign is changed when the slip velocity has large value (e.g. curve for oil in Fig 3). Therefore the methods are typically supplemented by some other slip control methods to avoid deadhesion control acts. A way to find out the maximum value is to derivate the adhesion coefficient according the slip velocity or wheel acceleration according the force that corresponds with a motor torque. When the derivation is positive an operating point is in the stable area of the characteristic. If the derivation is negative the operating point is in the unstable area of the characteristic and when the derivation is zero the operating point is in the peak of the characteristic. The method needs not to determine train velocity but the adhesion coefficient or wheel acceleration needs to be known. Wheel acceleration is calculated as the derivation of wheel velocity. The coefficient cannot be measured but the coefficient has to be estimated:

$$T_L = \frac{a}{s+a}(T_m - J_m s\omega_m)a \tag{2.13}$$

Where

T_L is estimated load torque,

J_m is a motor moment of inertia,

ω_m is a motor angular speed,

T_m is a motor torque and

a is a low pass filter cut-off frequency.

From estimated load torque the adhesion coefficient can be calculated. The disadvantage is that the methods work behind the maximum point in the characteristic and the method periodically works in the unstable area of the adhesion-slip characteristic. The method disadvantage is that it causes inconsiderable motor torque ripple that is undesirable.

C. Methods Based on Speed Controller

Method in the group uses a speed controller to achieve the maximum value of the tangential force. The control method based on speed controller can operate in any part of the adhesion-slip velocity characteristic. The method is different from other methods because the method does not use a torque controller to control the slip velocity as other methods. But the method uses a speed controller. Principle of the method is described in [21] in detail. The described method has improved control logic comparing with other methods.

D. Methods Based on the Adhesion-Slip Velocity Characteristic Slope Determination

The method in this group determines position of the operating point on the adhesion-slip velocity characteristic from the slope of the characteristic. The slope can be determined e.g. from the motor torque and motor angular speed phase frequency characteristic [17].

E. Indirect Methods

Indirect methods are based on another principle than the previous methods mentioned above. The methods are typically based on detection of dynamic motions. The adhesion-slip velocity characteristic in the linear part provides high damping of some dynamic motions but in the nonlinear part the damping decreases and in the unstable area damping is negative. On this principle a slip control method can be based. The typical dynamic motions are torsional vibrations between wheels on one wheelset or lateral accelerations. Another approach is described in [22, 23, 24] where the described method is based on noise analysis to detect high value of the slip velocity.

2.1.4 Fuzzy Logic Controller

FLC can sometimes outperform than traditional control system like proportional-integral-derivative (PID) controllers and have often performed either similarly or even better than human operators. This is partially because most FLCs are non-linear controllers that are capable of controlling real world systems (the vast majority of such system are non-linear) better than a linear controller can, and with minimal to knowledge about the mathematical model of the plant or process being controlled [25].

In its attempt to mimic human control action, FLC, whose structure is shown on Figure 2.6 is composed of four main components: fuzzifier, rules, inference engine, and defuzzifier.

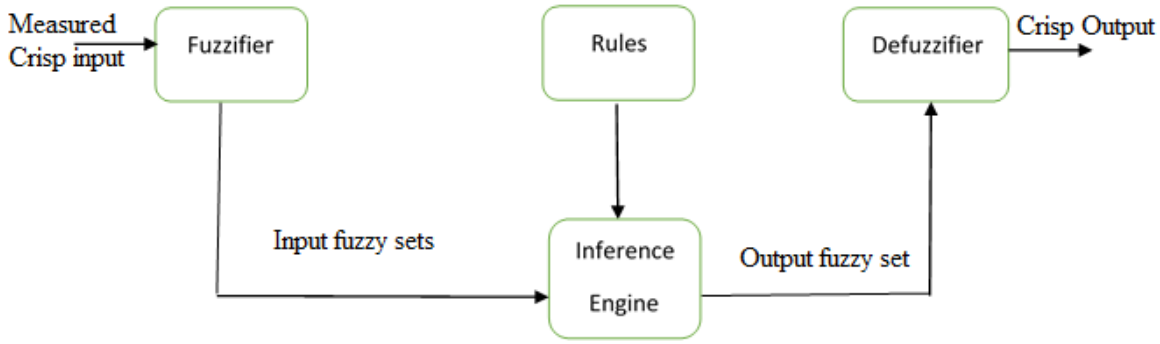

Figure 2.6 FLC Structure

The fuzzifier maps each measures numerical input variable in to fuzzy set. One motivation for doing this is that measurements may be corrupted by noise and are somewhat uncertain (even after filtering). So for example, a measured temperature of 26 ^{0}C may be modelled as the triangular fuzzy set that is symmetrically cantered around 26 ^{0}C where the base of the triangle is related to the uncertainty of this measurement. If, however, one believes that there is no measurement uncertainty, then the measurements can be modelled as crisp sets.

Rules have an if-then structure, for example, if temperature is low and pressure is high, then the fan is low. Each "if" part of a rule is called its antecedent, and the "then" part of a rule is called its consequent. Rules relate input fuzzy sets to output fuzzy sets. All of the rules are collected in to a rule base.

The inference engine decides which rules from the rule base are fired and what their degrees of firing are, by using the fuzzy set provided to it from the fuzzifier as well as some mathematics about fuzzy sets. The inference engine may also combine each rule's degree of firing with that rule's consequent fuzzy set to produce the rule's output fuzzy set (its fired-rule output set), and then combine all of those sets (across all of the fired rules), to produce an aggregated fuzzy output set using the mathematics of fuzzy sets; or it may send each rule's degree of firing directly to the defuzzifier where they are all aggregated in a different way.

The defuzzifier receives either the aggregated fuzzy output sets from the inference engine or the degree of firing for each rule plus some information about each consequent fuzzy set, and process

this data to produce crisp output that are then passed to the physical actuators that control the actual plant.

There are two widely used architectures for FLC that mainly differ in their fuzzy rule consequents. Mamdani FLC, developed by Mamdani and Assilian in which the antecedents and consequents of the rules are linguistic terms, If X1 is low and X2 is high, then U is low. The linguistic labels in a Mamdani FLC are represented by type-1 fuzzy sets (this method is used in this thesis work) [26, 27].

Takagi-Sugeno (TS) FLC or Takagi-Sugeno-Kang (TSK) FLC in which the antecedents of rules are also linguistic terms, but each rule consequent is modelled as a mathematical function of the input variables, for example: if X1 is Low and X2 is high, then u=g(x1,x2) where g(x1,x2) is a polynomial function of x1 and x2 (this can include a constant a linear or affine function, quadratic function etc)[26,28].

2.2 Related Works

Building a perfect slip controller is difficult due to the fact that railway vehicle's slip is a complex, non-linear and time varying process. Therefore, it is advantageous to use a non-classical methodology, like fuzzy logic based control systems. There are also several other non-classical methodologies like neural networks and evolutionary algorithms. The disadvantage with these methods is that they rely on numeric or measured data to form system models [3].

One major advantage with fuzzy logic is that it can include experienced human experts linguistic rules, describing how to design the slip control system. These linguistic rules are especially important when the access to measured data is limited. The reason is that they often contain information that is not included in the numerical values. These rules can be translated into if-then rules and in this form be included in the fuzzy logic algorithm.

M. Bauer and Masayoshi Tomizuka have done a remarkable research on road-traction slip controller using fuzzy logic. They did two fuzzy logic controllers. One controller which estimates the "peak-slip" corresponding to the maximum tire-road adhesion coefficient and regulates wheel slip at that value. The other one regulate brake torque to control wheel slip. The first controller was attractive because of its ability to maximize acceleration and deceleration regardless of road condition. However, they found through simulation that the controller's performance degrades in the presence of time-varying uncertainties [29]. The second one is found to be robust against changing road conditions and uncertainties. The target slip is predetermined and not necessarily the peak slip for all road conditions. If the target slip is set low, stable acceleration and deceleration is guaranteed regardless of road condition.

In other hand, Petr Pichlík and Jiří Zděnek used a speed controller to achieve the maximum value of the tangential force. The control method based on speed controller can operate in any part of the adhesion-slip velocity characteristic. The method is different from other methods because it does not use a torque controller to control the slip velocity as other methods [5].

Jianlong Zhang, Deling Chen and Chengliang Yin described a fuzzy Controller for Hybrid Traction Control System in Hybrid Electric Vehicles (HEVs) that prevents the spinning of the drive wheels during take-off and acceleration through targeted, brief brake impulses in motor torque. In the normal condition, the front wheels follow the control trace of the driver and rear

wheels follow the direction of the vehicle [30].The vehicle will spin and lose the control trace of the driver if the traction force is greater than the friction force. Therefore, a vehicle should maintain an adequate slip ratio of the tires and follow the control trace of the driver. The task is to have the fuzzy supervisory controller generate the electric brake torque, for motor of a HEV. The electric brake torque is treated as reference input regenerative braking torque, for lower level control modules. When these lower level motor controller tracks its reference input, the desired slip ratio, can be reduced. [8]

Chapter Three

Mathematical Modelling

Based on the theoretical concepts introduced under chapter 2, equation of motion for the quarter model of the rolling stock wheel-rail interaction can be expressed as equation 3.1 neglecting other disturbances moments.

$$J\dot{\omega} = -B\omega + T - T_a \tag{3.1}$$

Where J is inertia of the wheel

B is the viscous friction torque between the motor shaft and the wheel

T_a is adhesion torque

T is motoring torque

And longitudinal dynamic motion of the rail vehicle can be expressed using equation 3.2, by merging other disturbances under disturbance force.

$$M\dot{V} = F_t - F_a - F_r \tag{3.2}$$

Where:-

M is mass of the train

$\dot{V}$ is acceleration of the train

F_a is adhesion force

F_t is tractive force

F_r is disturbance force

In this work, the train vehicle is not physically modelled, instead only constant speed with small random due to the disturbance forces fluctuations is considered. These disturbance forces can be forces due to wind resistance, curving etc which makes the train slower or faster than the wheel speed, see figure 3.1.

On a sloped track surface. This movement is mathematically represented using a free-body diagram that describes all external forces acting on the train as shown in equation (3.2). There are resistance forces acting opposite to the train movement and are classified into frictional forces, air resistance and gravitational force, respectively. The resistance forces are represented in equation (3.3)

$$m_{dyn}\dot{V}_t = F_t - F_R \tag{3.3}$$

$$F_R = F_{roll} + F_{air} + F_{grad} + F_{crv} \tag{3.4}$$

Where

F_t is the tractive force of the train

F_R is the total resistance force of the train,

F_{roll} is the rolling resistance force

F_{air} is the aerodynamic drag force

F_{grad} is the gradient gravity force of the train

F_{crv} is the arc resistance

$\dot{V}_t$ is the acceleration of the train

m_{dyn} refers to the total effective mass of the train

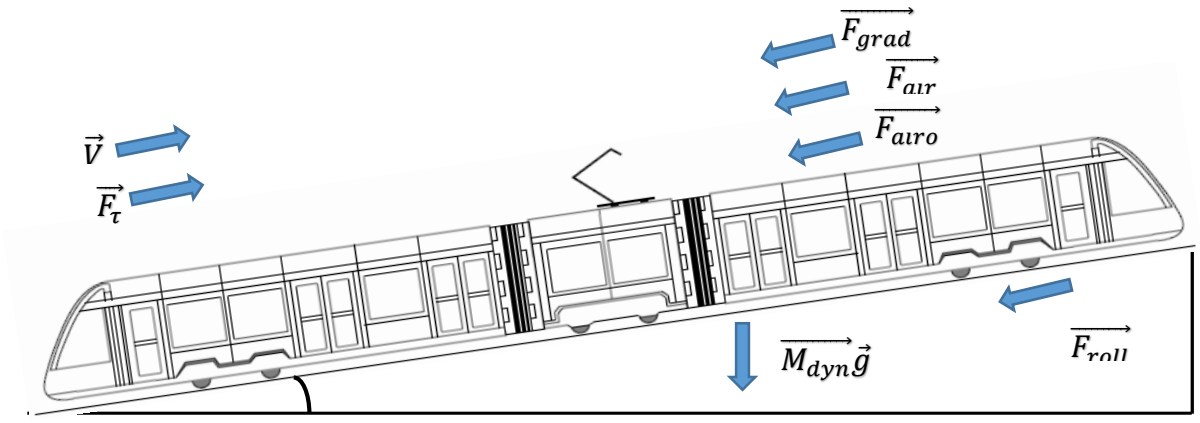

Figure 3.1 Longitudinal Dynamic of Railway Vehicle

Adhesion force (which is rolling force on the above picture) of the train model and adhesion torque of the wheel model can be related using equation 3.3.

$$T_a = R_w F_a \tag{3.5}$$

$$F_a = \mu(\lambda)N \tag{3.6}$$

$$N = Mg \tag{3.7}$$

Where: -

R_w is radius of the wheel

$\mu(\lambda)$ is adhesion coefficient as a function of slip ratio

M is mass of the train

g is gravitational acceleration

3.1 Adhesion Force Observer

Since adhesion force is a combination of complex variables, weight of the train, gravitational acceleration and adhesion coefficient (unmeasurable), it is better to design an effective observer which can calculate adhesion coefficient in real time based on estimated values. In control system theory, a state observer is a system that provides an estimate of the internal state of a given real system from measurement of the input and output of the system in real time.

From equation 3.1, speed loop using classical PI controller can be modelled as shown on figure 3.2. Where, ramp reference input is applied to represent acceleration of the wheel, PI controller to regulate the actual speed so that it can track the reference and the wheel rail contact as a plant to be controlled. The black blocks represent the physical systems modelled and the blue blocks are systems to be implemented on microcontroller.

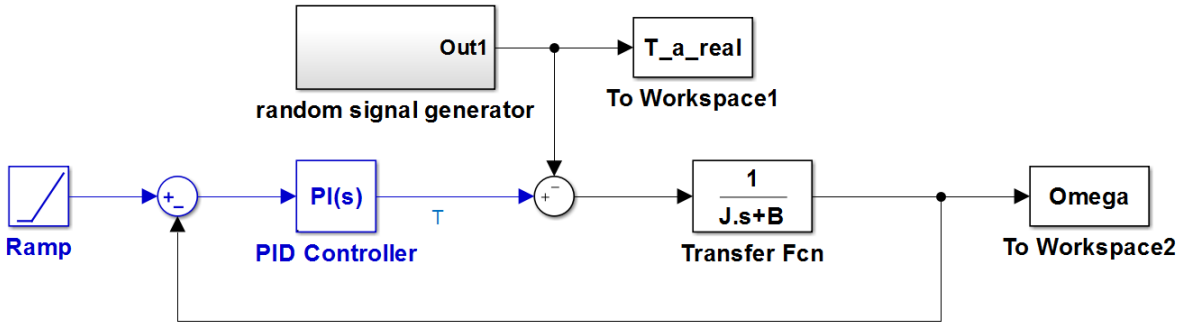

Figure 3.2. Classical PI Controller Speed Loop

From this model, the adhesion torque T_a can be expressed as

$$T_a = T - J\dot{\omega} - B\omega \tag{3.8}$$

Taking Laplace transform yields

$$T_a(s) = T(s) - Js\omega(s) - B\omega(s) \tag{3.9}$$

$$T_a(s) = T(s) - (Js + B)\omega(s)$$

Therefore it is possible to design similar loop which can observe the adhesion torque, hence the adhesion coefficient. The difference between the two loops is that, on the real speed loop the physical parameters are used in the black blocks while the estimated values are used in the blue blocks.

$$\widetilde{T_a(s)} = \widetilde{T(s)} - \left(\tilde{J}s + \tilde{B}\right)\omega(s) \tag{3.10}$$

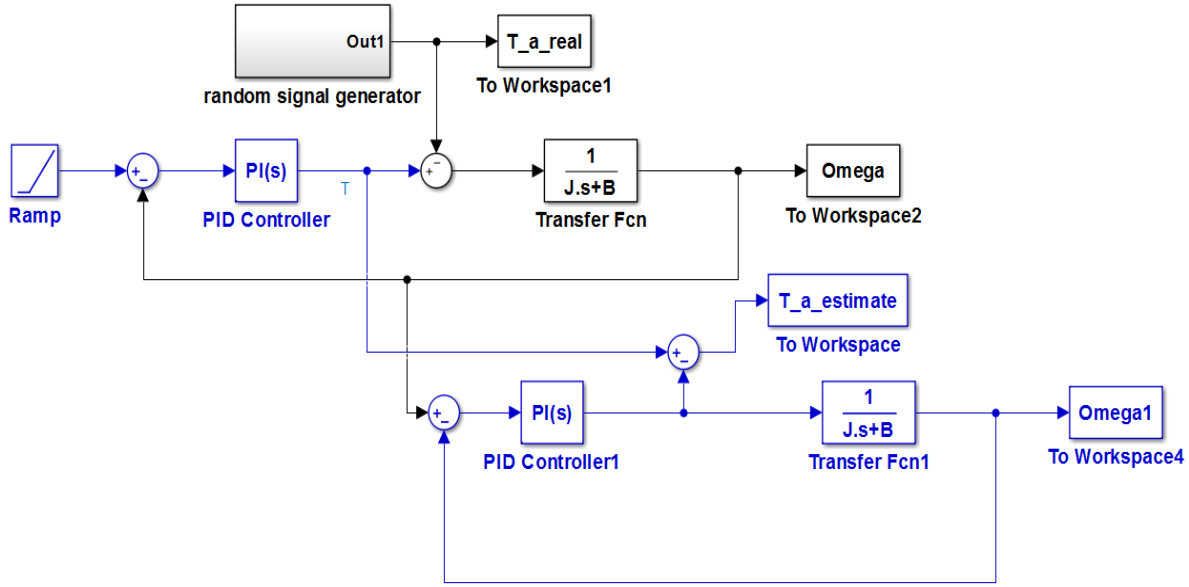

Figure 3.3 Adhesion Torque Estimator

The estimated adhesion coefficient $\hat{\mu}$ can be obtained by

$$\hat{\mu} = \frac{\widehat{T_a}}{N * R_w} \tag{3.11}$$

From the above wheel modelling, it is clear that the dynamics of the motor control are conditioned, not only by the nominal time of velocity increasing in set-point tracking mode, but also by load moment disturbances which excite electrical and mechanical natural frequencies. Therefore, a short control response time, or a large bandwidth is necessary to avoid the fastest disturbance phenomena; and also it is essential to damp them, and this requires that all natural frequencies are located within the control bandwidth. In the case of locomotive, the response time of the torque

control would have to be lower than ten milliseconds to be able to control the fastest phenomena [12]. Therefore the PI controller's coefficients are defined based on this concept.

Figure 3.3 shows adhesion torque estimator modelled on MATLAB Simulink with classical speed controller loop. The black blocks and signals represent real physical systems and blue blocks and signals represent programs to be implemented inside the microcontroller.

3.2 PI Controller Coefficients

PI controller can be represented using Laplace format of the proportional and integral terms using equation

$$PI = \frac{K_p s + K_i}{s} \tag{3.12}$$

Where K_p is proportional term constant

K_i is integral term constant

And the wheel model as a plant to be controlled can be represented as

$$\frac{1}{Js + B} \tag{3.13}$$

Therefore the open loop transfer function can be given as

$$G(s) = \frac{K_p s + K_i}{Js^2 + B} \tag{3.14}$$

The closed loop transfer function with unity feedback can be expressed as

$$G_c(s) = \frac{K_p s + K_i}{Js^2 + (B + K_p)s + K_i} \tag{3.15}$$

Which is similar with ordinary second order transfer function which can be expressed as

$$G_c(s) = \frac{1}{s^2 + 2\zeta\omega_n s + \omega_n^2} \tag{3.16}$$

Where ζ is the damping constant, which is about 0.707 for allowed bandwidth and 10% overshoot

ω_n is natural frequency, which is equal to the bandwidth pulse (rad/sec)

3.3 Burckhardt Static Modell (BSM)

As it has been discussed in chapter two, adhesion force and slip ratio can be related using the equation 3.17 using Burckhardt static model. Since it is a complex of different parameters which depends one another, it is modelled on MATLAB Simulink blocks as follows excluding the speed term. The final model of equation 3.17 is demonstrated as figure with subsystems to be discussed below.

$$\mu(\lambda) = \left[C_1\left(1 - e^{-C_2\lambda}\right) - C_3\lambda\right] \tag{3.17}$$

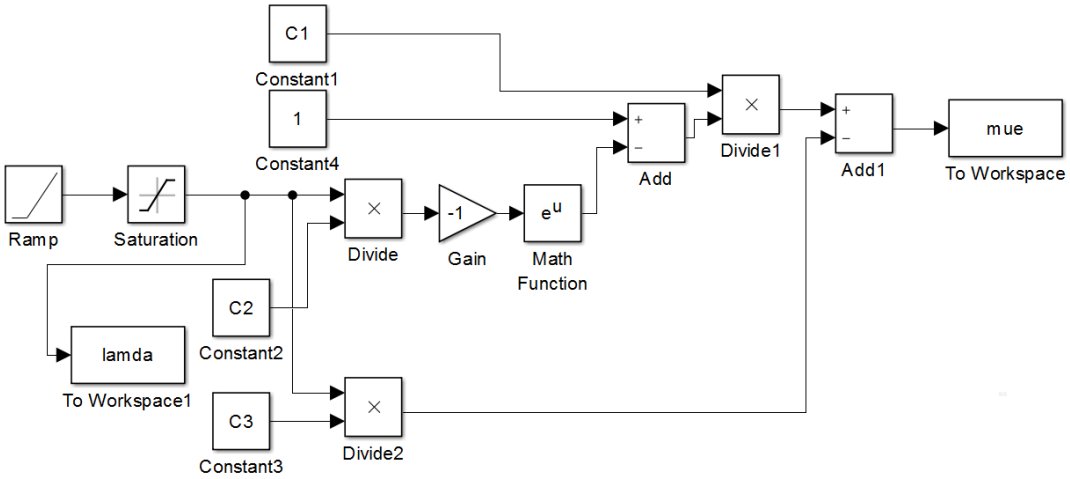

Figure 3.4 BSM MATLAB Model

As mentioned on scope of this thesis, train vehicle is not modelled as a physical system rather the slip ratio between the wheel and the train is modelled, see figure 3.5.

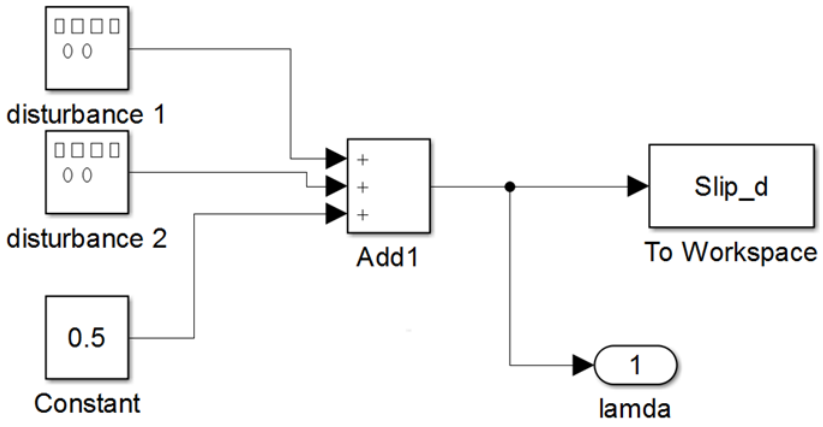

Figure 3.5 Slip Ratio Model

The ultimate aim of slip controller is to keep the slip ratio to constant value which provides the optimized adhesion coefficient and validate the controller performance by imbedding inside the classical PI speed controller. Figure 3.6 depicts, Simulink model of speed controller with adhesion torque as a load torque.

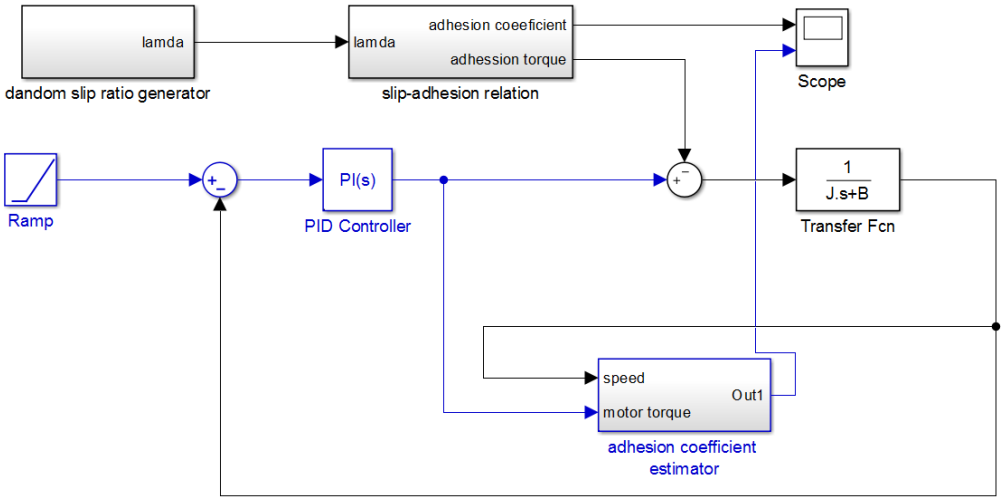

Figure 3.6. PI Speed Controller without Slip Controller

3.4 Fuzzy Logic Controller Design

The control objective of the slip ratio FLC controller is to maintain the wheel slip as close as possible to the fixed value. The fixed value of the slip has been distinguished to provide optimal friction between wheel and road surface under varying disturbance conditions. The closer the slip is to the fixed value the better the adhesion coefficient between the wheel and rail. This condition

is helpful to achieve stable operation of the train vehicles and effective utilization of power equipment.

FLC can easily adapt to changing rail irregularities, contaminant conditions, non-linearity in the vehicle system etc. the advantage of FLC is that, it is based on rule bases and membership functions for its design aspect. Whereas other type of controllers need linier or time invariant transfer functions between all input parameters and the desired output parameters. Comparing with switching or crisp value controllers, FLCs are effective because they consider grey areas values. Moreover, they are more robust and easier to implement as compared to classical control schemes.

3.4.1 The Fuzzy Inference System (FIS) Design of the Controller

For this thesis work, the fuzzy controller has two inputs, namely the error in slip, which is the actual slip minus the fixed slip ratio of 0.2, and the rate of change of this slip is the deceleration or acceleration of the rail vehicle. This deceleration of the vehicle changes with respect to time and is in sense real time simulated. The purpose of the controller is to maintain the vehicle slip as close as possible to the value of 0.2. From Chapter 3 we could see that the vehicle stability is maintained best when the actual calculated slip is maintained as close as possible to this desired value of 0.2. In this section, a set of fuzzy rules are defined to get the vehicle to operate in the stable range. Figure 3.7 shows the fuzzy inference system for slip controller.

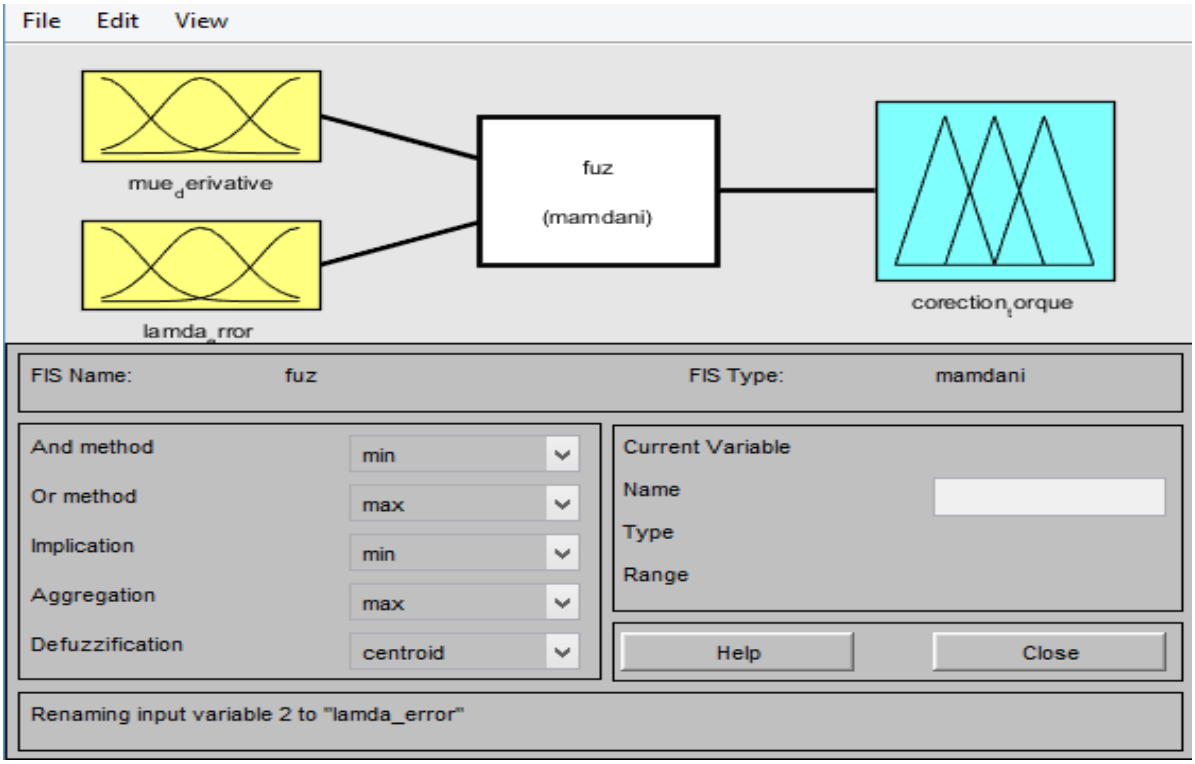

Figure 3.7 FIS Model for Slip Controller

Each input and output parameters are supposed to be assigned membership function.
Note that the nomenclature used for the membership functions is defined based on the following Fuzzy Set (FS) definitions.

- NB: Negative Big
- NS: Negative Small
- ZO: Zero
- PB: Positive Big
- PS: Positive small

Figure 3.8 shows the membership functions used for the input 1 which is the error in slip (the difference between 0.2 and current real time slip ratio). Memebrship process is illustrated on table 3.1 in which is based on real data's measured by [16]. the zero membership FS is exagurated in this thesis, because the simulation time is about one hour for contrasted value.

Table 3.1 slip ratio eroor membership

Memebership name	Type	Range
PB	Trim	[0.1, 1, 1]
PS	Trim	[0, 0.1, 0.15]
Zo	Trapmf	[-0.05, -0.05, 0.05, 0.05]
NS	Trim	[-0.15, -0.1, 0]
NB	Trim	[-1, -1, -0.1]

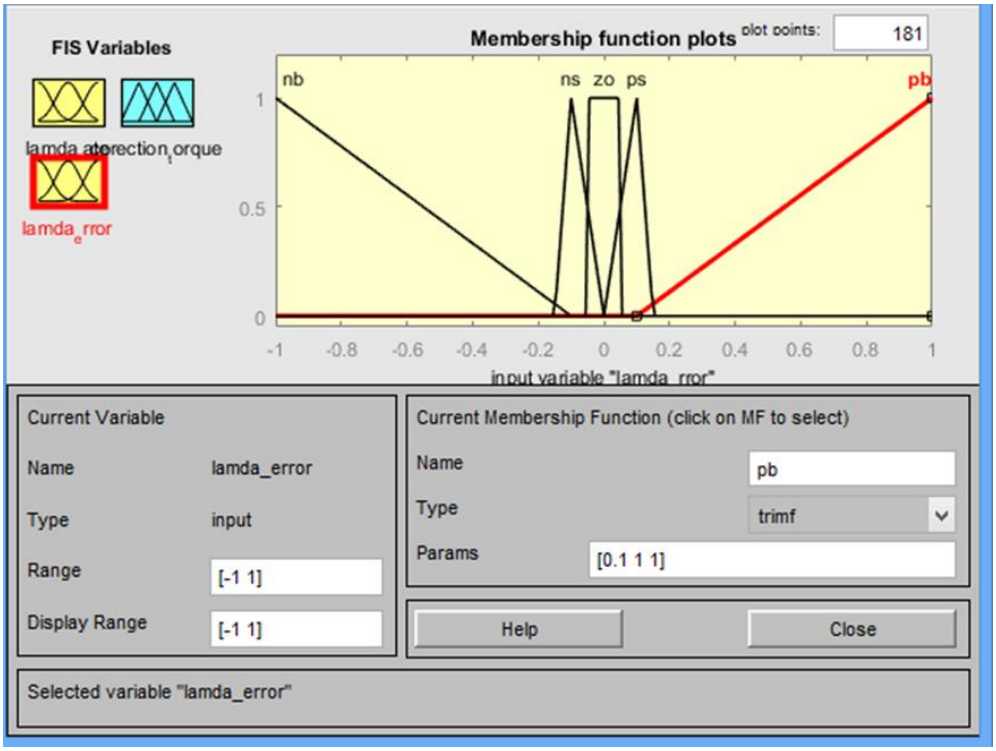

Figure 3.8 Membership Function of Input 1

Similarly, Figure 3.9 and table 3.2 shows Input 2 for the controller which is the rate of change of slip. It is the differential of the actual slip with respect to time. This is means acceleration of the train vehicle.

Table 3.2 Slip Ratio Eroor Derivative Membership

Memebership name	Type	Range
PB	Trim	[1.5, 10, 10]

PS	Trim	[3, 20, 20]
Zo	Trapmf	[-0.3, -0.3, 0.3, 0.3]
NS	Trim	[-20, -20, -3]
NB	Trim	[-100, -100, -15]

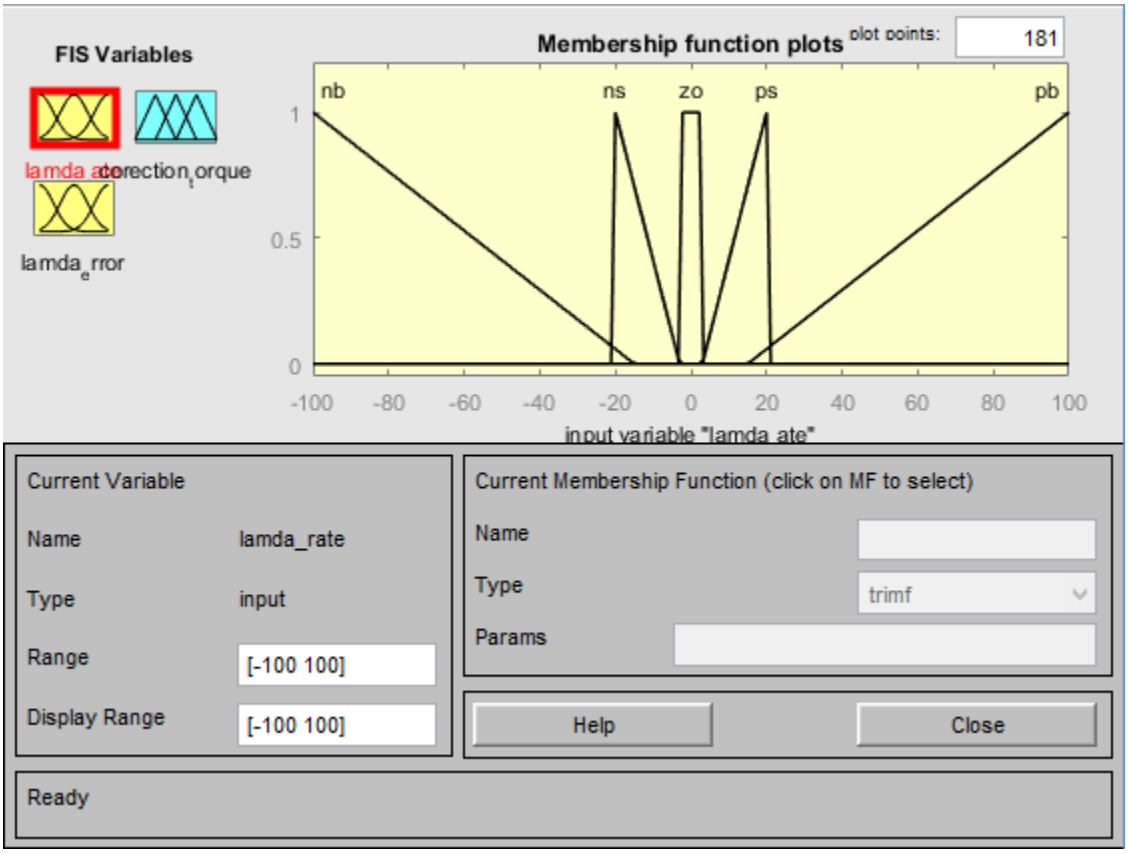

Figure 3.9 Membership function of input 2

Figure 3.10 is the output variable of the controller. The output in this case is the compensating adhesion coefficient which will be multiplied with normal load and radius of the wheel to be summed with controller output torque.

Table 3.3 Output Membership

Memebership name	Type	Range
PB	Trim	[0.5, 1, 1]

PS	Trim	[0, 0.5, 0.5]
Zo	Trim	[-0.05, 0, 0.05]
NS	Trim	[-0.5, -0.5, 0]
NB	Trim	[-1, -1, -0.5]

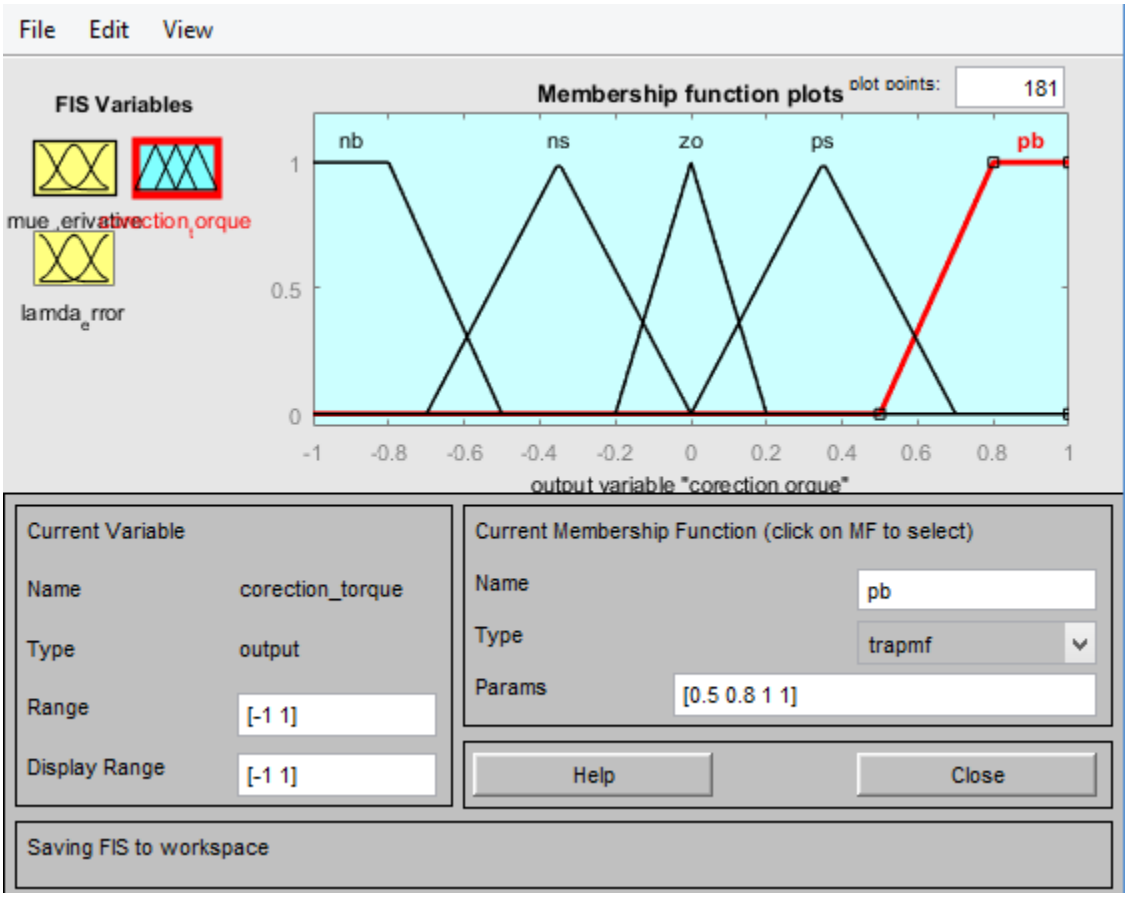

Figure 3.10. Output Variable of Fuzzy Controller

3.4.2 FIS Rule Base

The FLC has two inputs used, namely slip error and rate of change of slip error. The output of the controller is the compensation adhesion coefficient, which varies with corresponding changes of input variables. Five states are considered while forming the rule base, namely negative small (NS), negative big (NB), positive small (PS), positive big (PB) and zero (ZO). The rules for the

fuzzy controller is based on the following linguistic principles. These linguistic principles can be translated in to FIS using the Table 3.1

For the case of positive slip (acceleration case)

a. Positive slip error is means wheel speed is higher than it should be
b. Negative slip error is means wheel speed is less than it should be
c. Zero slip error is means wheel speed is at the desired point
d. Positive rate of slip error is means the slip error is increasing
e. Negative rate of slip error is means the slip error is decreasing
f. Zero rate of slip error is means the slip error is constant

Then the controller rule can be derived as

a. If slip error is positive and rate of slip error is positive, decrease compensation torque a lot.
b. If slip error is negative and rate of slip error is negative, increase compensation torque a lot.
c. If slip error is positive and rate of slip error is negative, decrease compensation torque a litle.
d. If slip error is negative and rate of slip error is positive, decrease compensation torque a little

Table 3.4 Membership rule

	Slip error					
Rate of slip error		PB	PS	ZO	NS	NB
	PB	NB	NB	NB	NS	ZO
	PS	NB	PS	NS	PS	PS
	ZO	NB	NS	ZO	PS	PB

	NS	NS	NS	ZO	PS	PB
	NB	NS	NB	PS	PS	PB

And the rule could be written as follows

1. When Slip Error is PB and rate of slip error is PB then the compensation adhesion coefficient is NB.
2. When Slip Error is PB and rate of slip error is PS then the compensation adhesion coefficient is NB.
3. When Slip Error is PB and rate of slip error is ZO then the compensation adhesion coefficient is NB.
4. When Slip Error is PB and rate of slip error is NS then the compensation adhesion coefficient is NS.
5. When Slip Error is PB and rate of slip error is NB then the compensation adhesion coefficient is NS.
6. When Slip Error is PS and rate of slip error is PB then the compensation adhesion coefficient is NB.
7. When Slip Error is PS and rate of slip error is PS then the compensation adhesion coefficient is NB.
8. When Slip Error is PS and rate of slip error is ZO then the compensation adhesion coefficient is NS.
9. When Slip Error is PS and rate of slip error is NS then the compensation adhesion coefficient is NS.
10. When Slip Error is PS and rate of slip error is NB then the compensation adhesion coefficient is NS.
11. When Slip Error is ZO and rate of slip error is PB then the compensation adhesion coefficient is NB.

12. When Slip Error is ZO and rate of slip error is PS then the compensation adhesion coefficient is NS.
13. When Slip Error is ZO and rate of slip error is ZO then the compensation adhesion coefficient is ZO.
14. When Slip Error is ZO and rate of slip error is NS then the compensation adhesion coefficient is ZO.
15. When Slip Error is ZO and rate of slip error is NB then the compensation adhesion coefficient is PS.
16. When Slip Error is NS and rate of slip error is PB then the compensation adhesion coefficient is NS.
17. When Slip Error is NS and rate of slip error is PS then the compensation adhesion coefficient is PS.
18. When Slip Error is NS and rate of slip error is ZO then the compensation adhesion coefficient is PS.
19. When Slip Error is NS and rate of slip error is NS then the compensation adhesion coefficient is PS.
20. When Slip Error is NS and rate of slip error is NB then the compensation adhesion coefficient is PS.
21. When Slip Error is NB and rate of slip error is PB then the compensation adhesion coefficient is ZO.
22. When Slip Error is NB and rate of slip error is PS then the compensation adhesion coefficient is PS.
23. When Slip Error is NB and rate of slip error is ZO then the compensation adhesion coefficient is PB.
24. When Slip Error is NB and rate of slip error is NS then the compensation adhesion coefficient is PB.
25. When Slip Error is NB and rate of slip error is NB then the compensation adhesion coefficient is PB.

Then the inference system generates triangular and trapezoidal membership based on the rules installed. Figure 3.11 shows how the fuzzy rules are distributed over the FS value.

Figure 3.11 Fuzzy Rules Distribution

After designing FIS, the controller output is tested using MATLAB simulation, see figure 3.12.

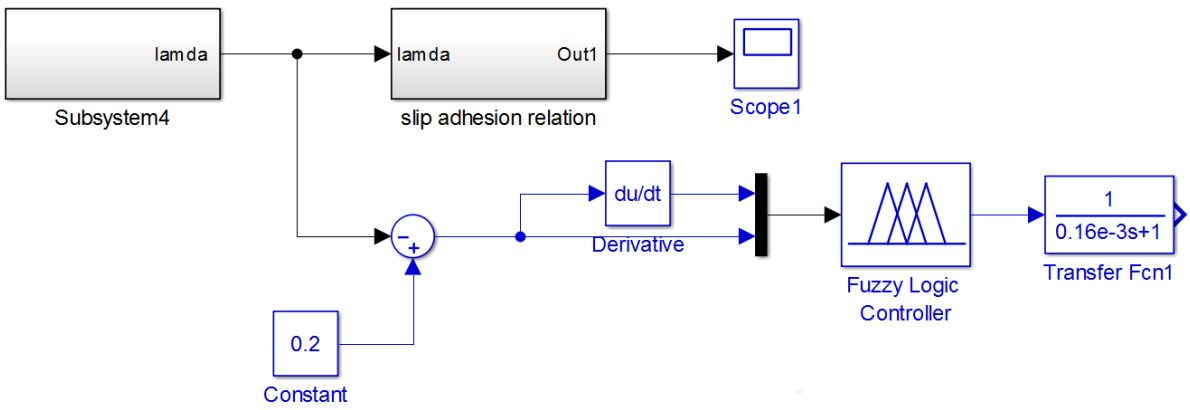

Figure 3.12 MATLAB Simulation of FLC

Low pass filter is attached to the output of the fuzzy controller in order to avoid rapid changes occur at the conflicting membership values. First order low pass filter can be modelled using equations 3.18 and 3.19.

$$\frac{1}{1+\tau s} \qquad (3.18)$$

$$\tau = \frac{1}{2\pi f_c} \qquad (3.19)$$

Where:-

τ is filter time constant

f_c is filter cut-off frequency

Then it is possible to apply the slip controller inside classical PI speed controller. Figure 3.13 shows the proposed FLC in order to control the slip ratio to constant value 0.2.

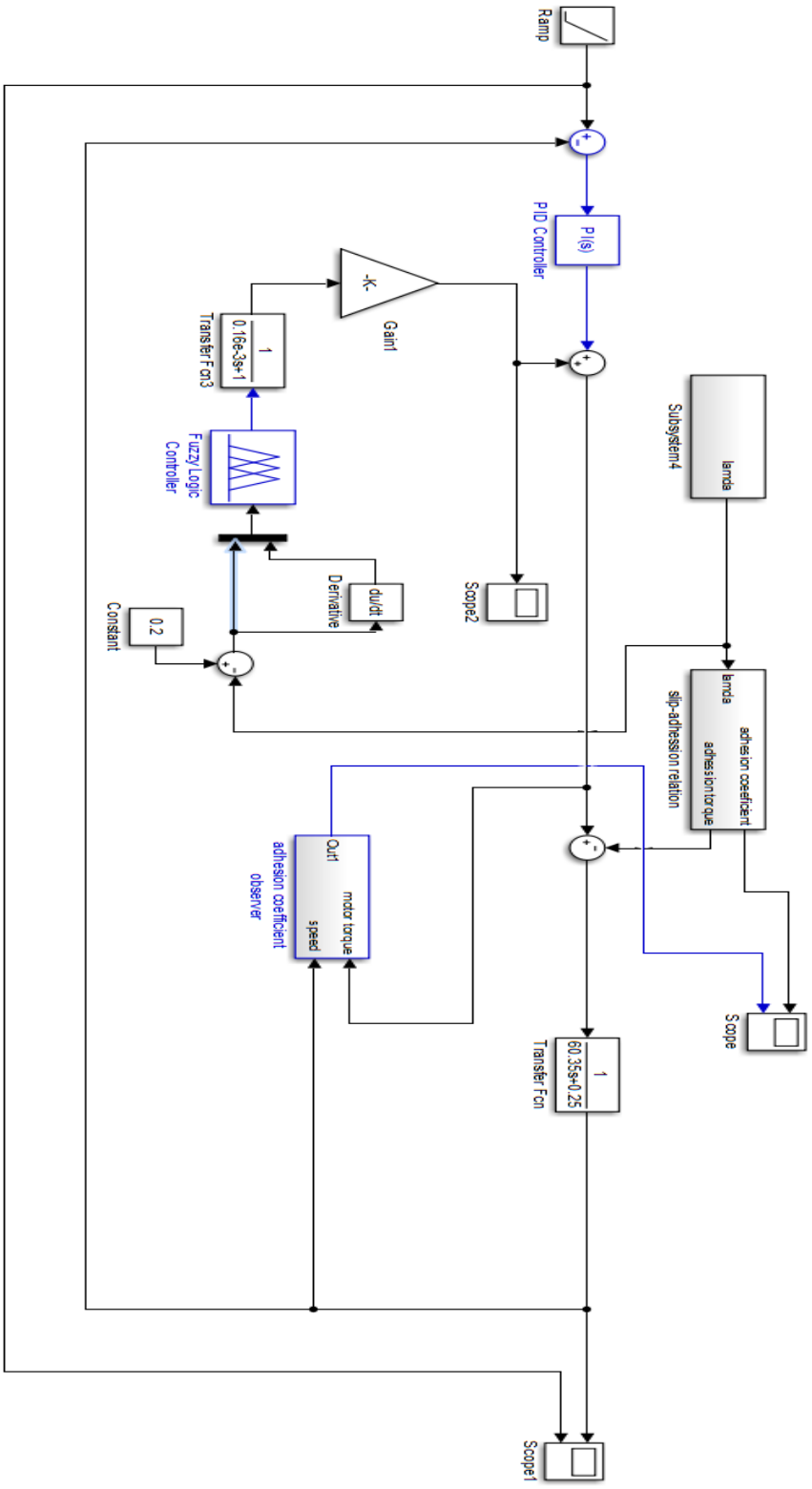

Figure 3.13 PI Slip Controller with FLC Slip Controller

Chapter Four

Simulation and Result Analysis

4.1 Adhesion Force Observer

For the adhesion force estimator modelled in chapter three, the estimator capability of tracing the original signal depends on, and the estimated variables accuracy and PI controller bandwidth. Table 4.1 shows physical parameters used for the model depicted on figure 3.1. Wheel mechanical property parameters are taken from [31], whereas controller and filter parameters are calculated as follows based on mathematical modelling in chapter three.

Table 4.1 Wheel-rail model parameters

Physical quantity	Notation	Value
Inertia	J	60.35 Kg-m^2
Viscous friction	B	0.25 N-m-sec
Filter time constant	τ	0.00025, 0.001 sec
Integral constant	K_I	5600
Proportional constant	K_P	31

For speed loop with 4Hz bandwidth system

$$\omega_n = 2\pi * 4Hz = 25\, rad/sec$$

There fore

$$K_i = \omega_n^2 * J = 25^2 * 60.35 = 38000$$

$$K_p = 2\zeta\omega_n * J = 2 * 0.707 * 25 * 60.35 = 2133$$

Assuming that switching frequency of motor inverter is 4 kHz, maximum possible bandwidth for the observer controller is 4 kHz. Applying random adhesion torque on the load side, the following results are collected for different filter bandwidths and estimated variables variation.

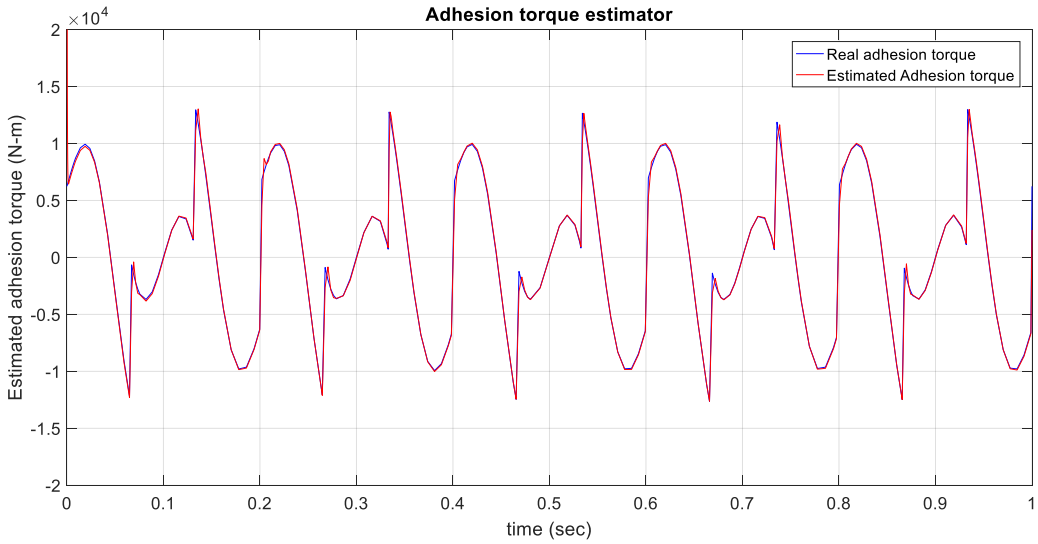

Figure 4.1 Adhesion Torque Estimation with 1 Khz Filter

Figure 4.1 shows how the original signal is traced with respect to the observed signal. For 1 kHz observer bandwidth and exact value of the estimated variables with physical parameters, the adhesion observer traces the signal perfectly without delay and attenuation. However, in practical application, 1 kHz observer is extremely exposed to noise susceptibility and signal aliasing for randomly varying inputs. Figure 4.2 is the result obtained for 0.25 kHz observer bandwidth, which somehow attenuate the amplitude of the observed signal.

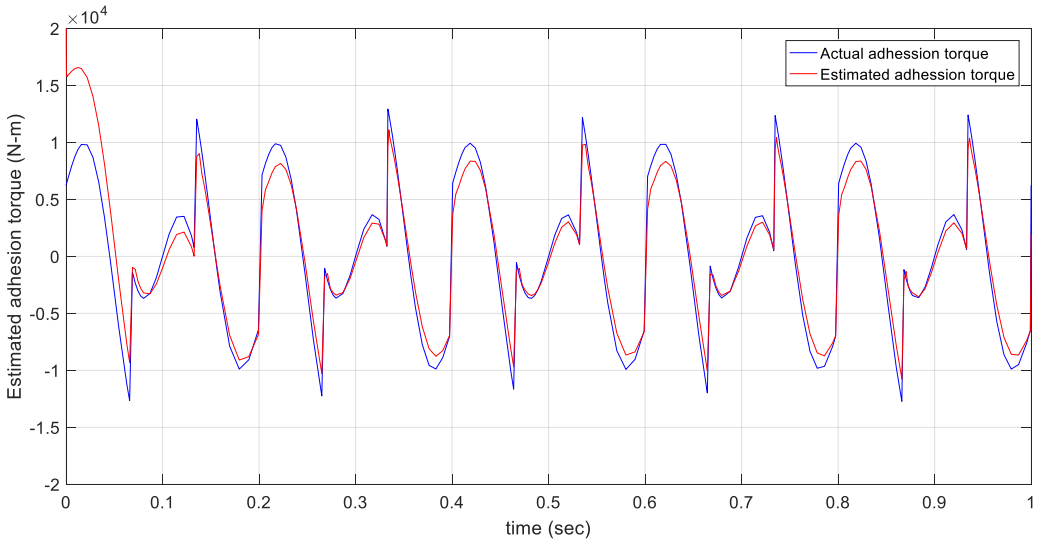

Figure 4.2 Adhesion Torque Estimation with 0.25 Khz Filter

In addition to filter bandwidth the other challenge of state observer comes through parameter estimation. Usually, values like inertia varies due to different uncertain conditions. For example in the wheel inertia case, the radius or mass of the wheel can reduce due to wearing. Figure 4.3 shows the adhesion force observer output compared with the original signal for wheel inertia reduced from 60.35 to 50.35 Kg-m^2

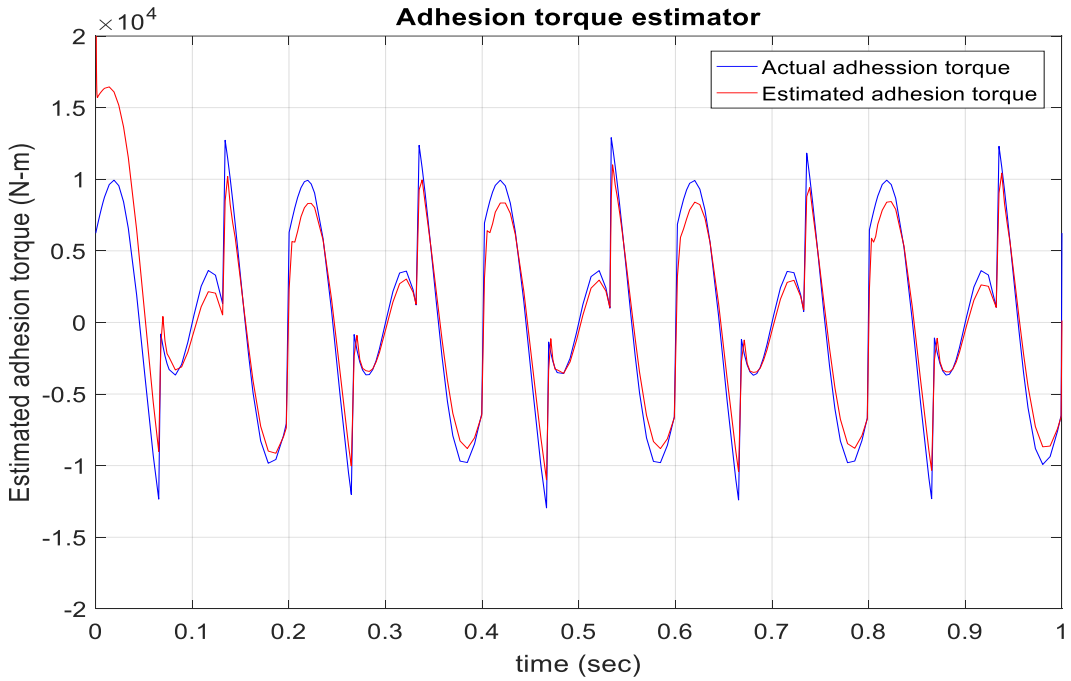

Figure 4.3 Adhesion Torque Estimation with J=50.35

From the three wave shapes, reduced filter bandwidth and estimated values variation causes deviation from the original signal. However this deviation is just amplitude attenuation and it can be compensated easily. Moreover, the deviation is not too much to accept the observation is wrong.

4.2 Burckhardt Static Modell (BSM)

Based on the mathematical modelling of the adhesion coefficient versus the slip ratio, the adhesion force depends on the slip variation according to selected BSM. Again, wheel mechanical property and continuum mechanics parameters are taken from [31] for simulation purpose as listed in table 4.1 table.

In addition coefficient of the magic formula are taken from the slip-adhesion curve shown on figure 2.2. In which

- C_1 is the maximum value of friction curve, which is assumed to be 0.8 at slip ratio equal to 0.2
- C_2 is the friction curve shape in the linear region is assumed to be 10, which is the slope of adhesion coefficient and slip ratio
- C_3 is the friction curve difference between the maximum value at $\lambda = 1$ is taken as 0.1 assuming the final settling point of the curve is 0.7

Figure 4.4 illustrates the value of adhesion coefficient for slip value from 0 to 1

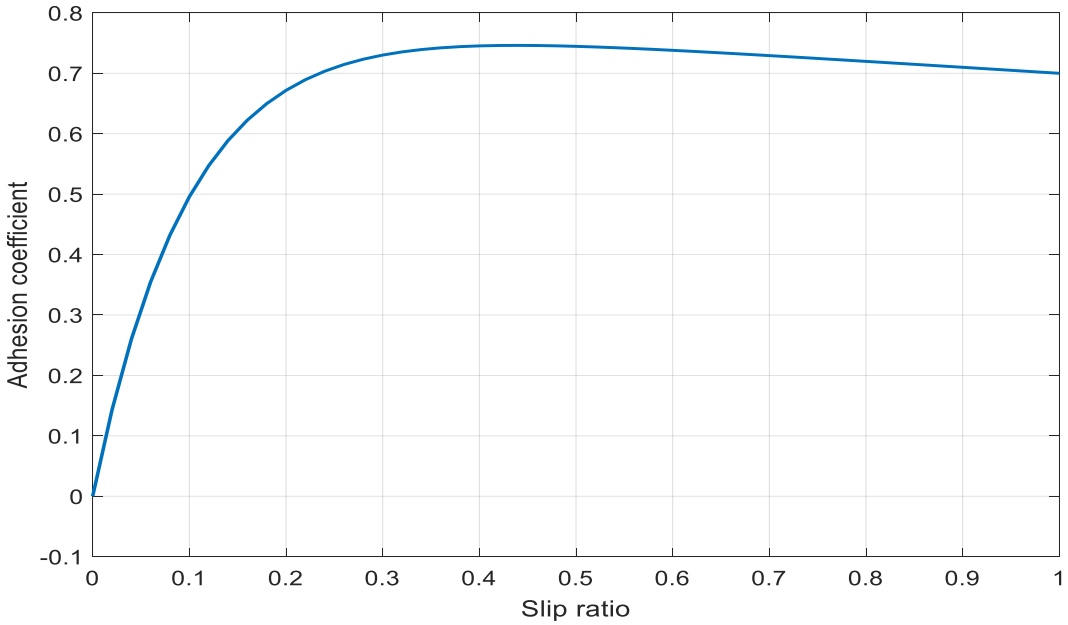

Figure 4.4 Adhesion Coefficient Variation with Slip Ratio

As figure 4.4 shows, the adhesion coefficient increases as the absolute value of slip ratio increase. Which means the load torque is randomly varying whenever there is random variation of longitudinal speed between the train and wheel. .

The PI slip controller modelled in chapter three, see figure 3.6, have speed response shown on figure 4.5 at no load. On this thesis, the speed response characteristics like overshoot and settling times are not point of interest. However, the effect of adhesion torque as a load torque varying with slip ratio is the most important one.

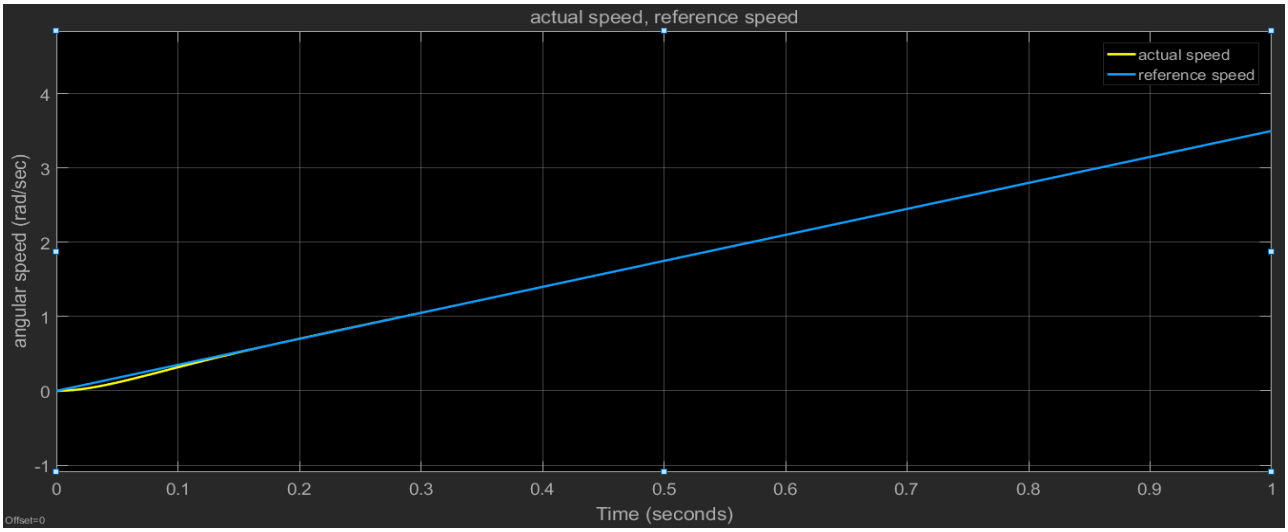

Figure 4.5 Speed Response of PI Controller at No Load

Now, let's consider the same PI speed controller model but with adhesion torque as a load. The speed response of this system for ramp angular wheel speed accelerating at 3.5 rad/sec2 for slip ratio between 0 and 1 as shown in figure 4.6 is given by figure 4.7.

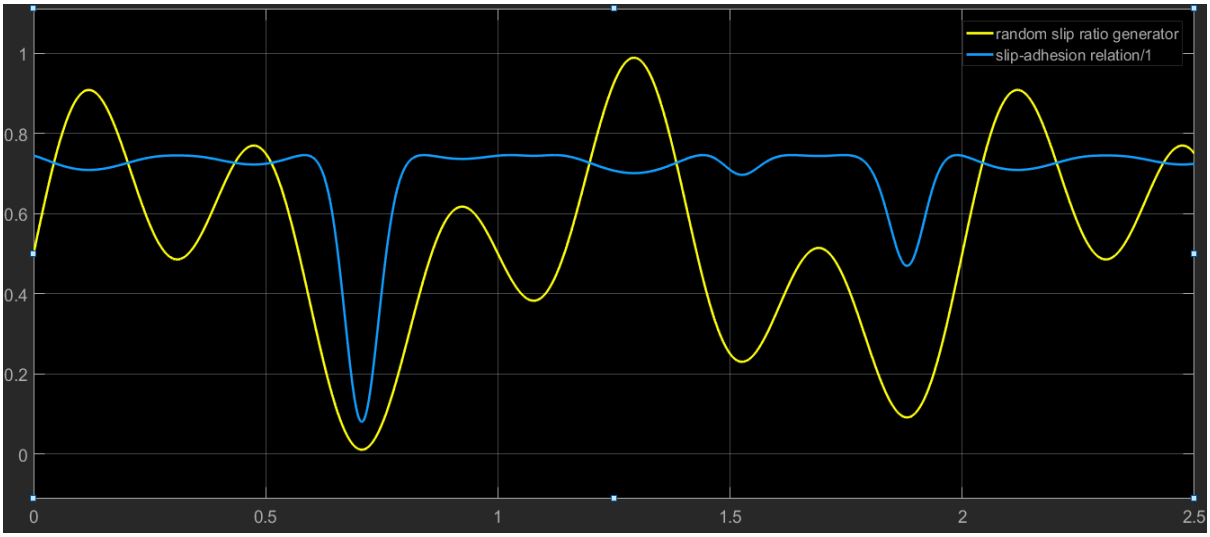

Figure 4.6. Adhesion Coefficient Variation with Random Slip Ratio

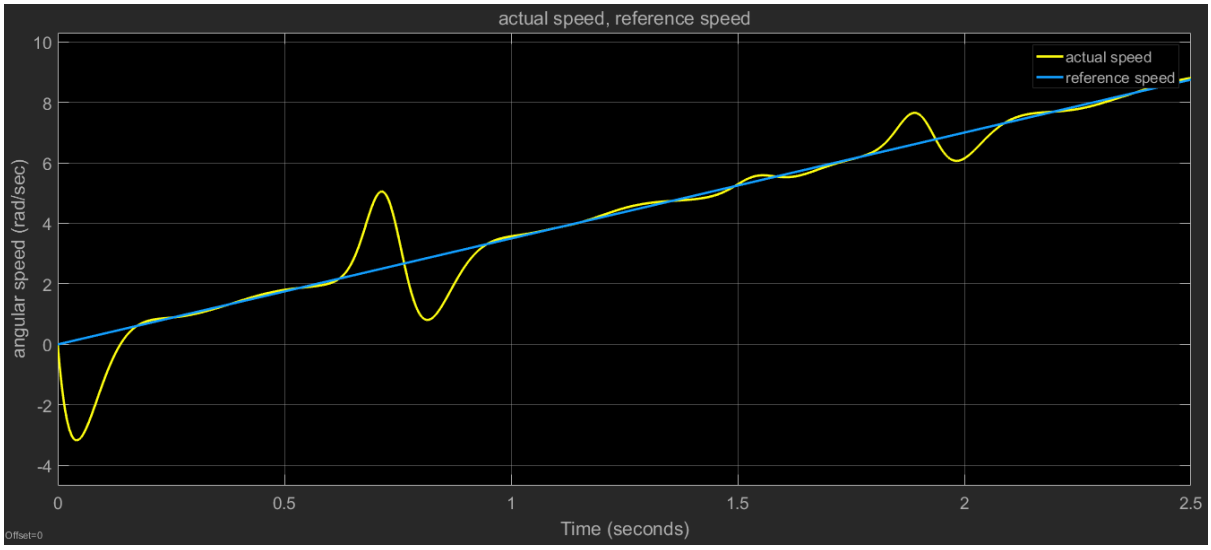

Figure 4.7 Speed Response of PI Controller with Adhesion Torque Load

The speed response is randomly fluctuating as the load torque is fluctuating randomly due to uncertain disturbances which has caused the slip ratio to oscillate. Therefore, it is important to implement slip controller which keeps the slip ratio at the optimal value which gives the maximum adhesion coefficient and stable operation.

4.3 FLC Slip Controller

By including FLC which controls vehicle slip inside the speed loop, it is possible to improve the speed response. For the same parameters used for section 4.2, FLC gives adhesion coefficient compensation parameter which will be multiplied with normal force of the train and wheel radius to give compensation torque. Figure 4.8 shows the output of the fuzzy controller to compensate the torque variation.

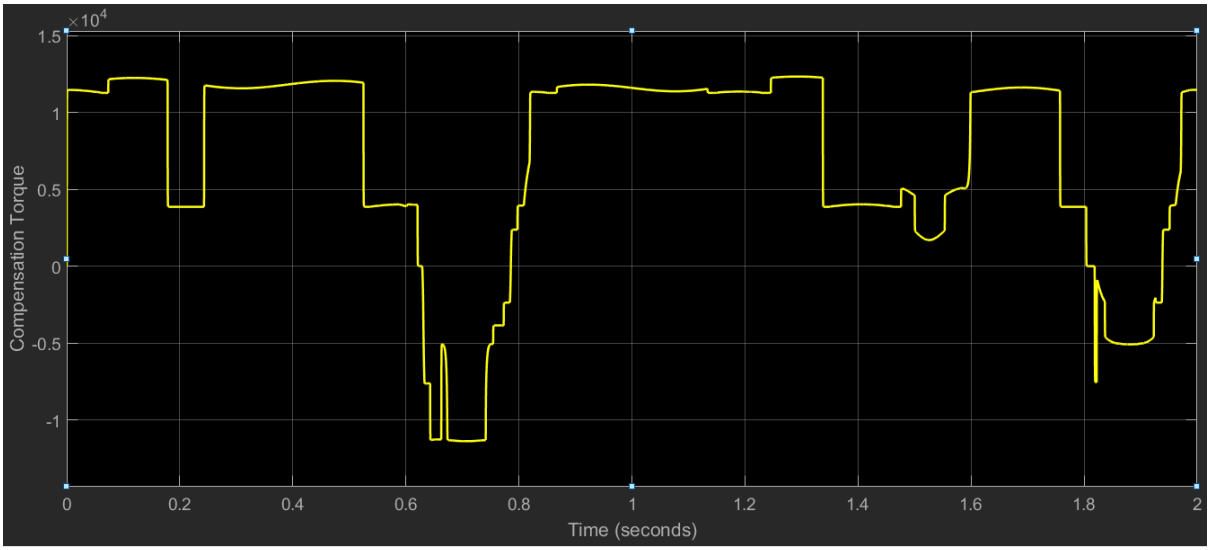

Figure 4.8 Compensation Torque

Based on this correction the speed response is improved as shown on figure 4.9.

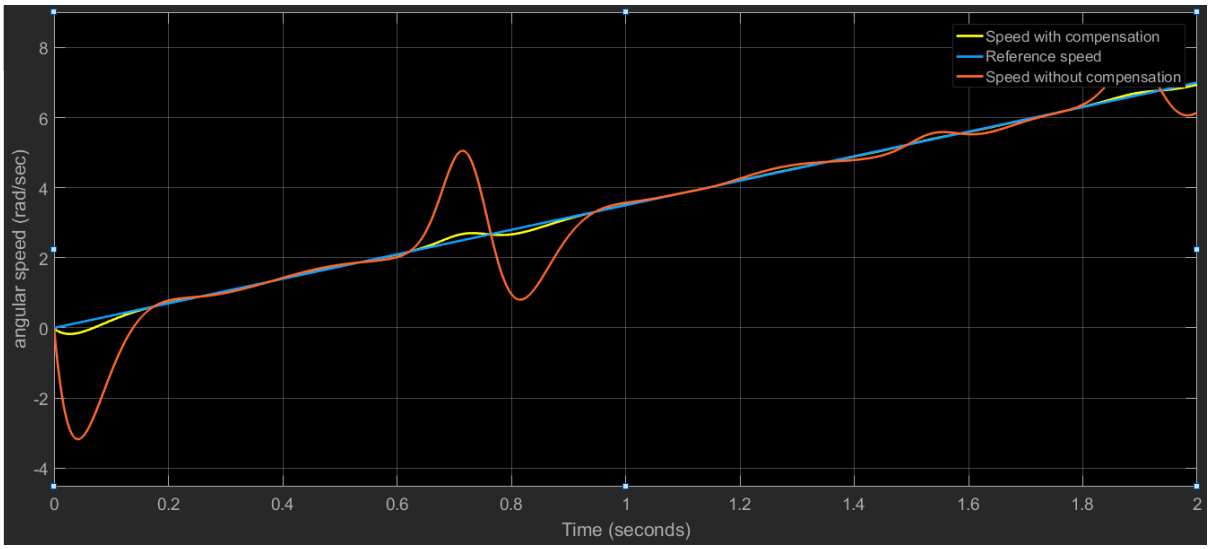

Figure 4.9 Speed Response with FLC

For example, at time 0.7 sec, the slip ratio is drastically declined from maximum point 0.75 to 0.01. Which in return causes the decrease in the adhesion force coefficient in the linier region. For this adhesion coefficient value, the speed output of the PI controller got overshoot up to 50% in early stage of the accelerating speed. Similarly during the slip maximization, the adhesion coefficient increases in the linear region and slightly decrease in the non linier region area. During this phenomenon, the speed of the wheel faces similar undershoot up to 50% in the early time of acceleration. However the overshoot and undershoot decrease up to 26% as the speed of the wheel increases. Using FLC slip controller the adhesion torque effect is reduced by compensating the traction torque. It reduces the wheel speed overshoot and undershoot up to 6% during positive acceleration.

Chapter Five

Conclusion and Recommendation

5.1 Conclusion

In this thesis automatic slip controller using a Fuzzy Logic Controller is designed in order to achieve optimized adhesion force between railway vehicle wheel and railroad. The main findings and outcome of this thesis work can be listed as follows.

Different slip controlling mechanisms are studied since the development of proposal. Then slip controller using speed loop method is chosen, in which the slip ratio is calculated from the longitudinal speed difference of driven and non-driven speed wheels. The slip ratio is controlled to constant value 0.2 which is found to be optimal value by other researches.

The main reason of controlling slip velocity is to control adhesion force constant which determines the transfer of applied moment on the wheel in to tangential force. The relation between slip ratio and adhesion coefficient is complicated because of certain and uncertain factors. From several models available, Burckhardt Static Modell (BSM) which is based on the magic formula is used to develop slip-adhesion coefficient curve.

Since it is difficult to measure the existing adhesion torque between the wheel and the rail, it is mandatory to design an observer which can trace adhesion torque based on estimated torque and mechanical property parameters. The designed observer's sensitivity is tested for variable estimated parameters and controller bandwidth. It has been found that using 1 kHz control loop bandwidth, the adhesion torque is perfectly traced without amplitude attenuation and phase shift. Whereas with small wheel inertia change and 0.25 kHz bandwidth, the observer shows slight amplitude attenuation.

After developing proper speed loop to control wheel speed, FLC based sleep controller is installed inside to compensate traction torque fluctuation caused by adhesion load. The FLC has two inputs namely the slip ratio error and the rate of slip ratio error. Using linguistic rules to increase and decrease compensating torque, the FLC generates adhesion coefficient which will be multiplied by the normal force and wheel radius to be added or subtracted from the traction torque.

Then the advantage of the controller is evaluated by considering the speed response with and without the slip controller. The result shows that overshoots and undershoots created by the adhesion load is compensated by the FLC to give smooth speed response. For the slip ratio varying drastically from 0.7 to 0.01 and vice versa, the wheel speed response shows up to 50% overshoot and undershoot in the early stage of the accelerating speed. However, the FLC slip controller compensates this up and down to 6% which is a remarkable result to smooth the motion of the system.

5.2 Recommendation

- During the work of this thesis, different literature resources are studied but none of them shows clear designing response methods well. For future work, it is better to focus on such research areas in order to improve railway resource utilization and customer comfort.

- On this thesis the simplest triangular FLC methods is used. It is true that there are other sophisticated but more accurate methods are available. For future work, it is advised to use methods like Gaussian membership. Moreover, the more the FLC is squeezed to ensure accuracy, the more the simulation time is. Therefore there should be code optimization in order to apply this design for real system.

Reference

1. N. Bosso et al. “mechatronic modelling of real-time wheel rail contact”, Springer-Verlag, Berlin Heidelberg 2013.
2. Jurgen Tomas, Mechanics of particle adhesion, Otto-von-Guericke-University, Magdeburg, Germany
3. Tomizuka, M.,and J. K. Hedrick. 1993. Automated Vehicle Control for IVHS Systems. Presented at IFAC Conference.
4. Daniel Frylmark and Stefan Johnsson, Automatic Slip Control for Railway Vehicles, Master’s thesis, performed in Vehicular Systems, Link¨opings universitet, 2003
5. Petr Pichlík, Jiří Zděnek, Overview of Slip Control Methods Used in Locomotives, CTU in Prague, FEE, Department of Electric Drives and Traction, Prague, Czech Republic, Transactions on Electrical Engineering, Vol. 3 (2014), No. 2
6. A.D. Cheok and S. Shiomi. Combined heuristic knowledge and limted measurement based fuzzy logic antiskid control for railway applications. IEEE Transactions on systems, man and cybernetics, 30(4):557–568, November 2000.
7. Park, S., H.; Kim, J.; Choi, J., J.; Yamazaki, H.;"Modeling and control of adhesion force in railway rolling stocks," Control Systems, IEEE , vol.28, no.5, pp.44-58, October 2008
8. Sung Hwan Park, Jong Shik Sim, Jeong Ju Choi, and Hiro-o Yamazaki, Modelling and control of adhesion force in railway rolling stocks, IEEE control systems magazine, october 2008
9. Kondo, K., "Anti-slip control technologies for the railway vehicle traction," Vehicle Power and Propulsion Conference (VPPC), 2012 IEEE , vol., no., pp.1306,1311, 9-12 Oct. 2012
10. T. Ohyama, “Some basic studies on the influence of surface contamination on adhesion force between wheel and rail at high speed,” Q. Rep. Railw. Tech. Res. Inst., vol. 30, no. 3, pp. 127–135, 1989.
11. S. Shirai, “Adhesion phenomena at high-speed range and performance of an improved slip-detector,” Q. Rep. Railw. Tech. Res. Inst., vol. 18, no. 4, pp. 189–190, 1977.
12. A. Kawamura, K. Takeuchi, T. Furuya, Y. Takaoka, K. Yoshimoto, and M. Cao. Measurement of the tractive force and the new adhesion control by the newly developed tractive force measurement equipment. IEEE, Proceedings of the Power Conversion Conference, 2:879–884, April 2002.

13. Slobodan N.Vukosavic, Digital control of electrical drives, The university of Belgrade, Slobodan N. Vukosavić University of Belgrade Faculty of Electrical Engineering Bulevar Kralja Aleksandra 73,11120 Belgrade, Serbia, 2007
14. Duengen, R. 1989. The Application of the COP888 to a 2-wheel ABS System. *Electronic Engineering*, Vol. 61, No. 748.
15. Mei, T., X.; Yu, J., H.; Wilson, D., A.; "Wheelset dynamics and wheel slip detection", STECH2006, Chengdu, China. 2006
16. C.Elmas, U.Guvenc and M.U.Dogan, Rail road friction coefficient estimation and experimental setup design of electric vehicle, Balkan Journal of Electrical and computer engineering, specialissue, 2015
17. Liu, J., Zhao, H., Zhai, W., "Mechanism of self-excited torsional vibration of locomotive driving system,", Front. Mech. Eng. China, vol. 5, no. 4. pp 465-469, 2010
18. Danzer, M. (2008), Elektrická trakce 7. Adheze (In Czech) [online], Available: http://www.kves.uniza.sk/kvesnew/ dokumenty/et/ET%20skripta%20Danzer/ETR700.pdf
19. Frylmark, D., and Johnsson, S., "Automatic Slip Control for Railway Vehicles," M.S. thesis, Dept. of Elect. Eng., Linkopings univ., Linkopings, Sweeden, 2003.
20. D. Frylmark and S. Johnsson, "Automatic Slip Control for Railway Vehicles,".Master's thesis, LiTH-ISY-EX-3366-2003, Linköpings universitet, Linköping, 2003.
21. M. Buscher, M.; Pfeiffer,. R; Schwartz, J., "Radschlupfregelung für Drehstrom-lokomotiven, " (in German) Elektrische Bahnen, vol. 91 no. 5, 1993, pp.
22. Mei, T., X.; Yu, J., H.; Wilson, D., A.; "A Mechatronic Approach for Anti-slip Control in Railway Traction", Proceedings of the 17th World Congress, The International Federation of Automatic Control, Seoul, Korea, July 2008
23. Liu, J., Zhao, H., Zhai, W., "Mechanism of self-excited torsional vibration of locomotive driving system," Front. Mech. Eng. China, vol. 5, no. 4. pp 465-469, 2010
24. Spiryagin, M.; Lee, K., S.; Yoo, H., H.; "Control system for maximum use of adhesive forces of a railway vehicle in a tractive mode," Mechanical Systems and Signal Processing 22, pp 709-720, 2008.
25. Takagi, T. – Sugeno, M.: Fuzzy identification of systems and its application to modeling and control, IEEE Trans. Systems, Man and Cybernetics, 15, 1985, pp. 116-132

26. R. Palm and K. Storjohann. Torque optimization for a locomotive using fuzzy logic. *Proceedings of the 1994 ACM symposium on Applied Computing*, pages 105–109, April 1994.
27. Wang, L. W. 1992. Stable Adaptive Fuzzy Control of Nonlinear Systems. Proceedings of the 31st Conf. on Decision and Control.
28. Kandel, A., and G. Langoholz. 1994. *Fuzzy Control Systems*, CRC Press, Boca Raton.
29. M. Bauer Masayoshi Tomizuka, Fuzzy Logic Traction Controllers and Their Effect on Longitudinal Vehicle Platoon Systems, California PATH Research Report, UCB-ITS-PRR-95-14
30. Jianlong Zhang, Deling Chen and Chengliang Yin, Adaptive Fuzzy Controller for Hybrid Traction Control System based on Automatic Road Identification, Institute of Automobile Engineering Shanghai Jiao Tong University N0. 800, Dongchuan Rd.,Minhang District, Shanghai, China
31. S. Uchida, "Brake of railway III," Japan Train Oper. Assoc. J. Brake of Railway Vehicles, vol. 3, pp. 25–28, 2001.